

Date: 06/15/2015

## EIC Calorimeter Detector R&D Progress Report

**Project ID:** eRD1

**Project Name:** EIC Calorimeter Consortium

**Period Reported:** from 01/01/15 to 06/15/15

**Project Leaders:** H.Z. Huang and C. Woody

**Contact Person:** H.Z. Huang ([huang@physics.ucla.edu](mailto:huang@physics.ucla.edu)) and C. Woody ([woody@bnl.gov](mailto:woody@bnl.gov))

### Collaborators

*S.Boose, J.Haggerty, J.Huang, E.Kistenev, E.Mannel, C.Pinkenberg,  
S. Stoll and C. Woody*  
(PHENIX Group, Physics Department)

*E. Aschenauer, S. Fazio, A. Kiselev*  
(Spin and EIC Group, Physics Department)

*Y. Fisyak*  
(STAR Group, Physics Department)  
Brookhaven National Laboratory

*F. Yang, L. Zhang and R-Y. Zhu*  
California Institute of Technology

*T. Horn*  
The Catholic University of America and  
Thomas Jefferson National Accelerator Facility

Wouter Deconinck  
College of William & Mary

Zhiwen Zhao  
Duke University

Guy Ron  
Racah Institute of Physics, Hebrew University of Jerusalem

W. Jacobs, G. Visser and S. Wissink  
Indiana University

*C. Munoz-Camacho*  
IPN Orsay, France

Tim Holmstrom  
Longwood University, Farmville

*S. Heppelmann*  
Pennsylvania State University

*C. Gagliardi and M.M. Mondal*  
Texas A&M University

**Alexandre Camsonne**  
**Thomas Jefferson National Accelerator Facility**

***L. Dunkelberger, H.Z. Huang, K. Landry, Y. Pan, S. Trentalange, O. Tsai***  
**University of California at Los Angeles**

***Y. Zhang, H. Chen, X. Chen, Y. Guo, C. Li, Z. Tang and L. Zhou***  
**University of Science and Technology of China**

**Kai Jin, Nilanga Liyanage, Vincent Sulkosky, Nguyen Ton, Xiaochao Zheng**  
**University of Virginia, Charlottesville**

***H. Mkrtychyan***  
**Yerevan Physics Institute**

## Overview

This report describes the progress of the EIC Calorimeter R&D Consortium for the period 01/01/15 – 06/15/15. The EIC calorimeter consortium has major R&D efforts in these directions: 1) Development of a compact Tungsten powder and scintillating fiber (W/SciFi) based ElectroMagnetic Calorimeter (EMCal); 2) Evaluation of Silicon Photomultipliers (SiPMs) as a calorimeter readout sensor and its radiation hardness under expected EIC environment; 3) Development of a crystal detector at EIC with current focus on PWO crystals and a small effort on continuation of our previous BSO crystal evaluation; 4) collaboration with the EIC simulation group to develop calorimeter requirements and a quantitative estimate of EIC radiation environment. We are very pleased that a team led by Professor Xiaochao Zheng from UVa has joined the calorimeter consortium. The proposed new effort focuses on simulations and prototyping of a Shashlyk EMCal, in particular the investigation of production of scintillator plates using 3D printing technology.

On the W/SciFi detector development, we continue to improve the detector construction technique and improve the labour efficiency. We produced a new prototype detector designed for high energy resolution of  $6\%/\sqrt{E}$ . The prototype was tested at FNAL in a test run in May 2015. We found out two issues with the prototype: the light yield is significantly lower than we expected; and the filter plate used for uniformity in light collection worked as expected in creating a uniform response, but it also introduce significant light loss. We propose to resolve these technical issues and carry out a second prototype construction next year.

We continue to share the W/SciFi construction technology among the consortium and with an industrial partner, in anticipation that the real construction of the EIC calorimeter will take many more resources and much more manpower that a single institution can provide. At the same time we are also exploring construction techniques that will allow us to build 2-D projective calorimeter. The 2-D projective geometry, though not required for an EIC detector because of low event multiplicity, is desired for a RHIC detector like sPHENIX whose detector components could be used in the EIC era as well.

We continue to evaluate the performance of SiPMs and develop a cooled, temperature controlled operating system for SiPMs in order to achieve gain stability. We also propose to evaluate an APD readout option. A possible system test in the RHIC environment with a sizeable prototype EMCal array including a full readout, trigger and DAQ is under discussion within the consortium.

For the PWO crystal detector development, testing infrastructures have been developed at several institutions and characterization measurements have been carried out. The groups seek to consolidate these tests and understand the systematics from the different measurements. The measurements for radiation hardness of the PWO crystals from SICCAS have also yielded promising results. Potential new vendor for PWO crystals, CRYTUR, delivered one full size (20 cm) PWO crystal using their growth method.

For the BSO crystal development, a FNAL testing run was carried out. The USTC group is working on the calibration and simulations of the detector to extract a possible characterization of the detector performance despite the poor electron beam quality at FNAL. It is likely that another electron beam test, possibly at SLAC, is needed to determine the characteristic performance of the crystals. The FNAL test run was a parasitic effort to the STAR HCal test.

The proposed detector R&D effort from the team led by Professor Xiaochao Zheng is a major addition to the Calorimeter Consortium. The Shashlyk type EMCAL has excellent detector performance and can be made in fully projective geometry. The proposed simulations and possible innovative construction techniques using 3D printing technology are worthy of support. The new team will add a new dimension to our current R&D portfolio and will make the Consortium stronger when we move towards an EIC detector TDR in future years.

The budget request for FY2016 from the Calorimeter Consortium is below. Details and update will be presented at the meeting.

W/SciFi EMCAL Development Teams (UCLA team \$101.8 k, BNL team \$27 k)	\$128.8 k
SiPMs Test and Evaluation	\$23.0 k
PWO Development Team	\$75.0 k
Shashlyk EMCAL Team	\$60.2 k
Total	\$287.0 k

**Sub Project: Progress on Tungsten Powder Calorimeter R&D at UCLA**  
**Project Leader: H.Z. Huang and O. Tsai**

**Past**

**What was planned for this period?**

- Investigation of options for a high-resolution EMCal in the outgoing electron direction. This was a follow up of a global optimization of the EIC detector. In the first year of this program we planned to build a new EMCal prototype to learn the limitations of the technology and test it with the test beam at FNAL.
- Continued development of a compact light collection scheme for the W powder ScFi SPACAL type detector. This follows from a successful test run at FNAL in March of 2014 to further improve the light collection uniformity.
- Investigation of options for the ‘industrialization’ of production for W powder ScFi type calorimeters.

**What was achieved?**

We build a new EMCal prototype consisting of 16 towers, shown in Fig. 1. The transverse size of the detector was  $10 \times 10 \text{ cm}^2$ , with an active volume length of 25 cm (compared to 17 cm in our previous forward EMCal detector). We used 0.4 mm diameter scintillation fibers, spaced 0.667 mm apart. Composition of the absorber was 75% W powder and 25% Sn powder. Technology-wise, these parameters are probably very close to the practical limit for this particular method of building fiber calorimeters. We found that compared to our previous prototypes, it is more difficult to pack long thin fibers through a set of screens with such fine granularity due to friction between fibers. We used a vibrating platform to perform packing of fibers through the meshes, which was not needed for previous configurations. It was also difficult to spot missing holes during packing because the melted ends of the fibers essentially cover the entire mesh surface. Out of 25000 fibers, we missed 4 during packing, which were discovered only after the ends of the modules were machined (one of these missing fibers can be seen in the top left superblock of the new prototype as a black dot in the middle of the superblock). The packing of absorber into the fiber matrix and impregnation of the final assembly with epoxy was very similar to previous prototypes. Despite of a significant increase in the volume of the new prototype, there were no problems with mold release and with thermal runaway during epoxy curing. Unfortunately, due to miscommunication with the machine shop, both ends of the new prototypes were cut to the depth of the absorber/fiber mixture instead of the fiber/epoxy volume, as with all our previous detectors. This is required for good optical coupling. This mistake led to damages on the tips of some of the fibers, which we were not able to correct since this was one of the last operations in construction of this detector immediately prior to the test run. Interestingly, machinability of the composite absorber is quite different compare to pure W powder absorber. Previously we attempted to develop a technique to cut the absorber fiber structure without damage to the fiber in order to simplify the construction technique

and were unsuccessful. It was found that the tungsten particles significantly damaged some of the fibers, with potentially 100% loss of light. With the composite absorber (W/Sn) we did not observe similar damage in the new EMCal prototype- instead smudges of what looked like Sn on the surface of some of the fibers were observed under the microscope. Unfortunately, we have not yet been able to find a method to clean these smudges.

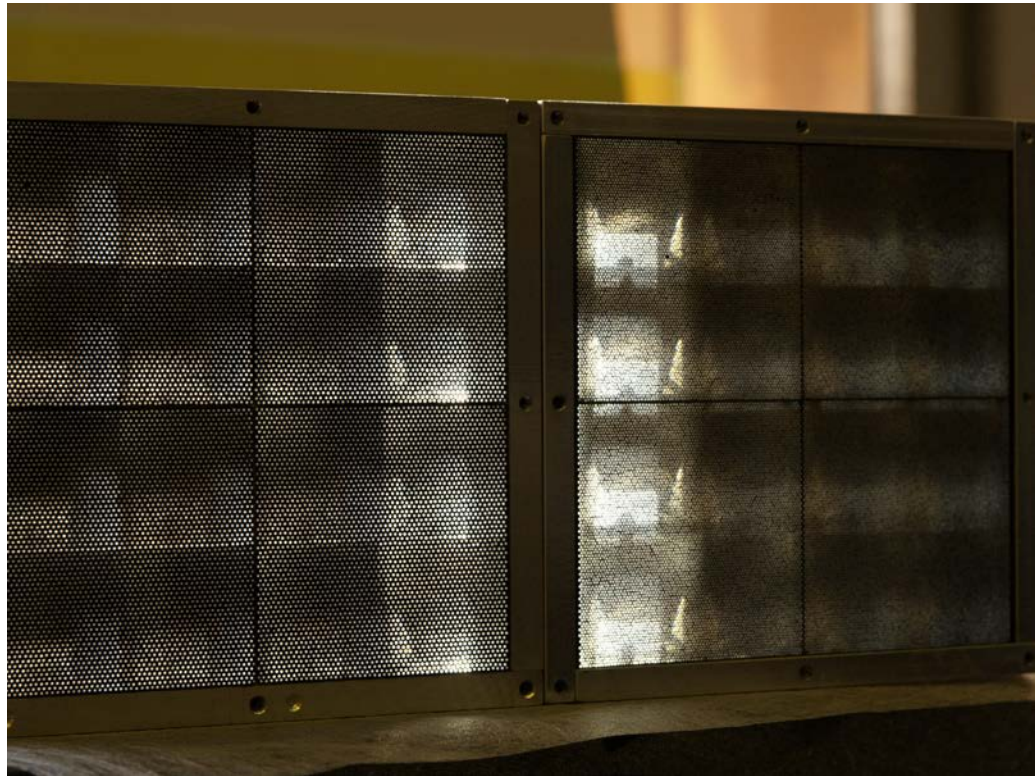


**Figure 1. Two EMCal prototypes, seen from the side opposite to readout. The new EMCal prototype has much finer sampling frequency compare to the old detector.**

Both prototypes were equipped with a new light collection scheme. A neutral density filter was designed to compensate for the non-uniform light collection observed in the 2014 test run. The design is based on the results of scanning of the old EMCal

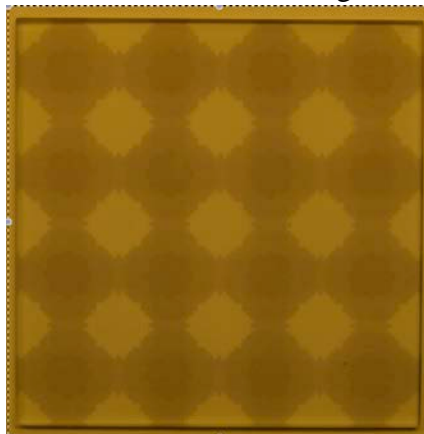


**Figure 2. A compensation filter for sixteen EMCal towers.**

prototype with an UV LED as was presented in our previous report. Commercially available direct printing of dye on acrylic plates seemed to work fine, although due to time constraints we were not able to perform mechanical stress tests on these components. The dye is stable and is not dissolvable by epoxy. The filter shown in Fig. 2 for an entire super module (16 channels) was printed on a 3 mm thick acrylic plate and then sandwiched by gluing to a 1.3 mm thick acrylic plate to protect the printed area (yellowish cast on Fig 2. is due to poor white balance of the camera). The transmittance of the filter plate alone is 85% (overall) and was verified with a laser. This filter

plate was glued at the tips of both EMCal prototypes and then individual light guides were glued to this filter plate. The overall process is quite tedious. In the future, we plan to change the method. In principle, the light guide and filter can be casted as a single block. The filter itself can be made from reflective mesh with the desired pattern. Then the light collection block will allow for easy integration of the LED monitoring system in the same manner that was done for the 2014 prototype, where the last mesh facing light guides were mirrored to allow light from a monitoring fiber to bounce back to the readout SiPMs. But the cost of a molding form precludes such an approach at this stage of the development.

Both prototypes were tested at FNAL at the end of May (May 19- May 29), 2015. As of June 10, 2015 we are still analysing the test beam results. The energy resolution of the new EMCal prototype was averaged over an impact area of approximately  $4 \times 4 \text{ cm}^2$  (active area of the scintillation hodoscope). No corrections were applied, i.e. the energy is a simple sum of all energy in 16 EMCal towers. As shown in Fig.3, the blue points are the raw experimental data, the red points are corrected for beam momentum spread, the magenta points are the ideal MC, and green points are expectation from MC with measured photo-statistics during the test run.

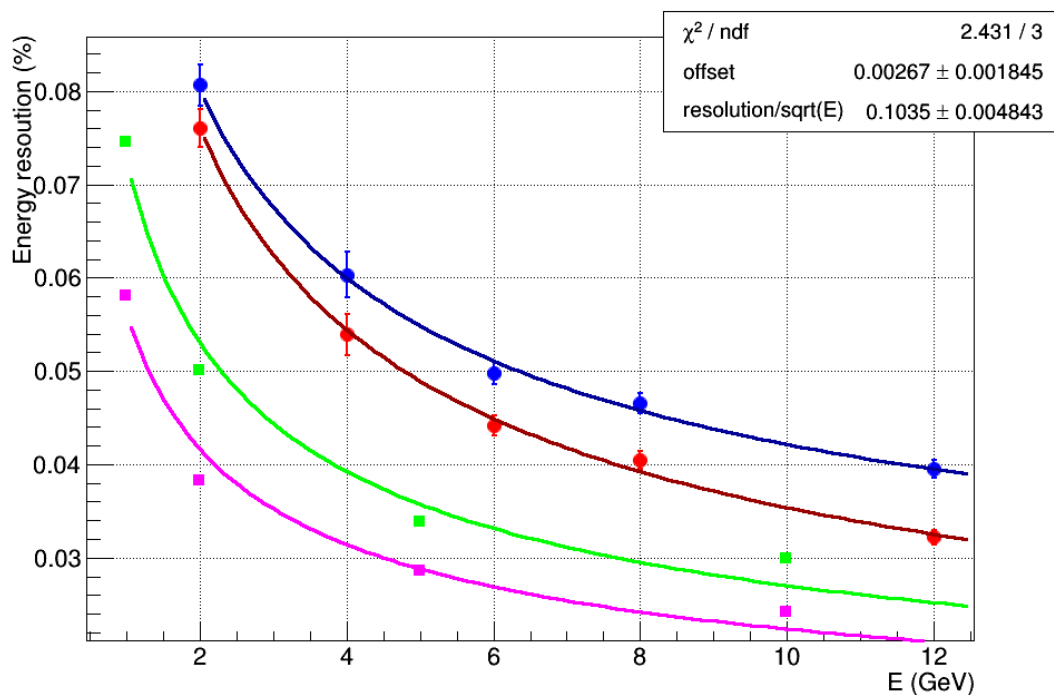


**Figure 3. Energy resolution in EM prototype compared with MC expectations: Blue – raw data; Red – with correction for beam energy spread; Green – MC expectation with measured photo-statistics; Magenta: Expectation from ideal MC.**

The first surprising result from the test run was the low light yield (LY) from the new detector of about 460 p.e./GeV. Prior to the test run, the expected LY was at the level of approximately 700-800 p.e./GeV, which was obtained from scaling the increased sampling fraction with respect to prototypes tested in 2014 and accounting for losses due to the filter. We ruled out that the attenuation length in thin fibers may be a potential problem by measuring the attenuation length in the fibers with 120 GeV protons and 4 GeV electrons during a longitudinal scan of the detector, as shown in

Fig.4. In both cases, the attenuation length obtained was close to what was measured in previous prototypes. According to MC simulations, an attenuation length of 75 cm or greater has a negligible effect on energy resolution. As in previous years the far ends (opposite to SiPMs) of scintillation fibers were painted with a white, diffusive paint.

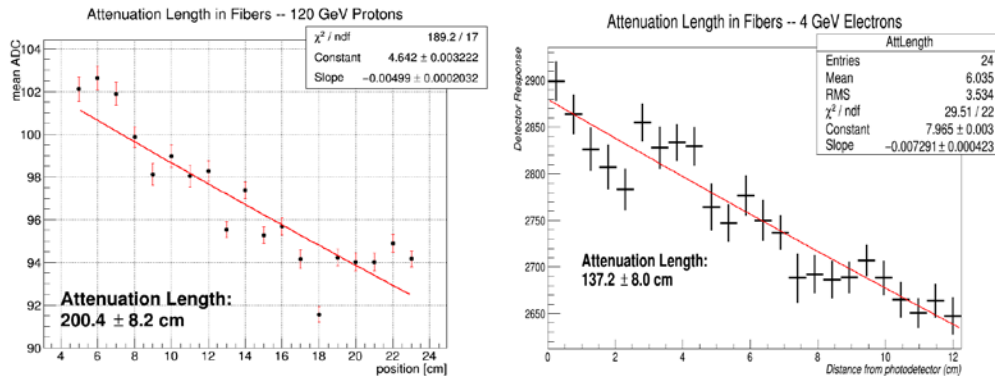


Figure 4. Attenuation length in 0.4 mm scintillation fibers measured in the test run.

We also compared the LY in our old prototype. Instead of the expected 15% loss in light yield due to a filter, we observed a 30% loss. At this moment we have not had any time to investigate the cause of this difference (our equipment is still in transit from FNAL to UCLA). During the summer we plan to do additional measurements with the light collection scheme to find what caused the loss of light to be more than expected. Possible causes include three additional layers of epoxy which were not present during initial measurements of the transparency of the filter plate. Spare filter plates make it possible for us to investigate this in the laboratory.

The uniformity of response from 4 GeV electrons across the face of the new detector is shown in Fig. 5. The impact points were selected with a scintillation hodoscope. The black lines show boundaries between superblocks (each superblock consists of a 2 x 2 tower array). The last row of the scintillator hodoscope was excluded because of side leakage from the ECal. The 'local' variations of response (within an area of 5 x 5 mm<sup>2</sup>) are around 2.3%, which are higher than the 1.4% measured in the previous prototype equipped with PMT readout and long light guides (for such measurements in the future we will need a large scintillator hodoscope).

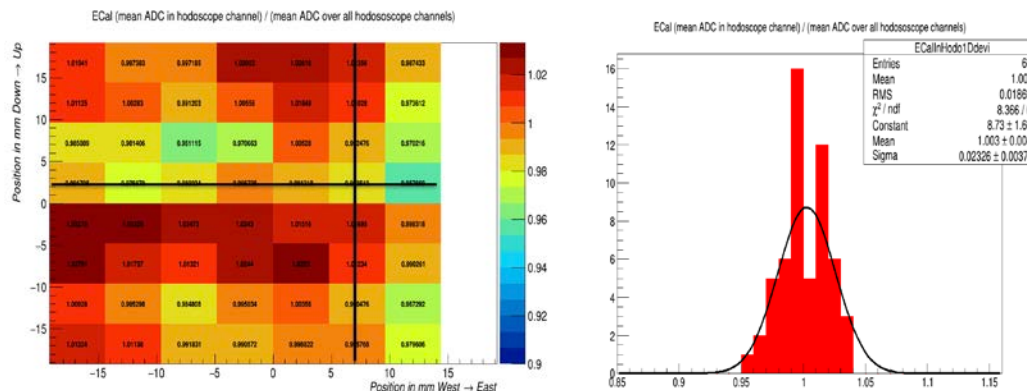
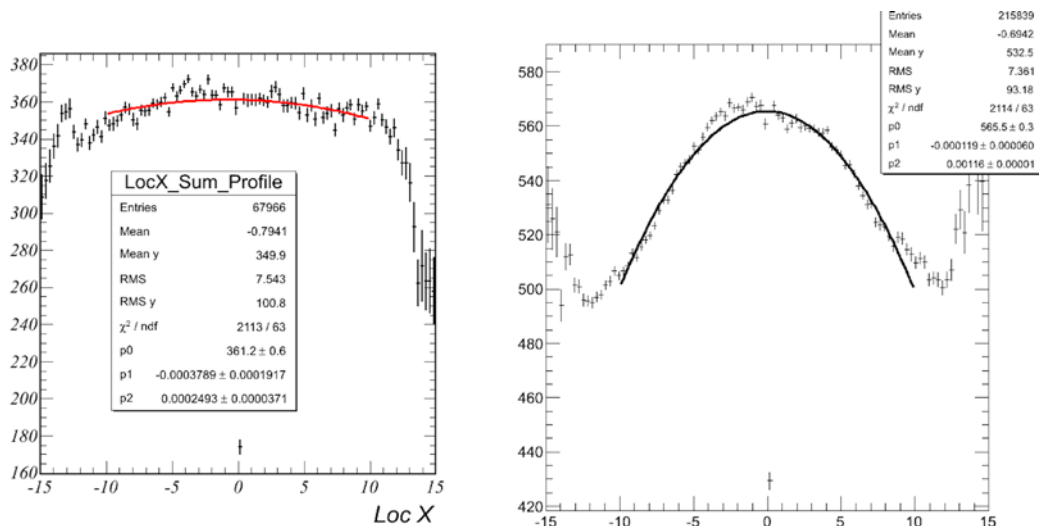


Figure 5. The uniformity of response across the face of the detector is 2.3% for 4 GeV electrons.

The exact cause of this increase in variation is not clear. Potentially a combination of possible damage to fibers during the production, variation of the absorber and imperfections in the filter can lead to the increase. We will perform additional measurements with the new EMCal prototype in the lab during this summer to shed more light on the possible cause.

The compensation filter did flatten response for both prototypes, as we expected. In Fig. 5 and Fig. 6 responses of the old EMCal prototype to 4 GeV are compared with and without the compensation filter. However, as mentioned earlier, we also lost more light than expected.



**Figure 6. Responses of the old EMCal prototype to 4 GeV electrons vs impact point. Left 2015 data with the filter, right 2014 data without a filter.**

All new data shown above are preliminary; analysis of test data is continuing as of June 15, 2015.

The technology of building EMCal calorimeters utilizing powders and scintillation fibers continues to be improved every year as within the EIC Calorimeter Consortium. For barrel 1D projective towers, we significantly simplified our assembly methods and reduced the required production time, as compared to the 2014 effort at UCLA. BNL and UIUC groups are investigating options for fully projective (2D) modules as well as mastering/improving the construction of 1D blocks developed at UCLA. The THP Company, a possible vendor for outsourcing major production task, is developing their own method of building 1D projective towers, with the first samples currently being shipped to BNL for inspection.

### **What was not achieved, why not, and what will be done to correct?**

The energy resolution of the new prototype is only slightly better than for the old EMCal prototypes. The big difference (red and green curves in Fig 3) between MC and data needs to be understood, as well as the reasons for the mediocre light yield. Measurements in the lab will help to clarify some of the possible problems, but to fully address all these questions we will need additional measurements with the test beam. The approach we want to pursue is as follows: We want to simplify things and avoid ambiguities when a few new developments are pursued together at one time (as

was done last year). First we want to tweak the parameters of the new matrix a bit more with MC simulations. It will be beneficial (technology-wise) to increase diameter of the fibers slightly from the present 0.4 mm. We want to postpone for now the usage of a composite absorber and will use pure W powder for a second prototype construction. We also want to use a simple PMT readout (ideally a single large photocathode area PMT for an entire block of 16 towers). In this way ambiguities we have with the present detector can be resolved. If we find a simple way to switch to a compact readout system for this new prototype during a test run, we can then test both readout methods in a single test run.

## **Future**

We plan to continue the development of powder/fiber technology for a high resolution EM calorimeter for the outgoing electron direction. In the second year our focus will be to address questions arising from the 2014 test run results and to determine whether this is the right technology for high-resolution EM calorimeters. This is consistent with our original plan of devoting about two years to pursue this development. The compact readout for barrel and hadron-side EM calorimeters will be refined in the future and improvements in construction techniques are a continuing effort. With every new prototype being constructed, our construction methods are becoming more and more efficient.

We also plan to initiate a new multi-year program for the EIC calorimeter consortium. We propose to construct and install a sizeable EMCal and HCal prototype detector in possible available space of STAR experimental hall. These prototypes will be used for future developments and testing of front-end electronics, trigger, DAQ, slow control and monitoring/calibration components. RHIC provides unique opportunity to test all these components in a realistic experimental environment before EIC starts. Such an on-site testing facility will extremely valuable when we develop the final TDR and construction of the calorimeter for EIC.

We wish to emphasize that the operation of a large scale prototype detector in a collider environment could have a major impact on the final performance of the designed detector. The CMS EMCal detector readout using thin APD, for example, experienced major problem due to the so called Nuclear Counting Effect (NCE) when the LHC started operation. The problem was attributed to direct ionization of the active silicone layers of the CMS APDs which was later supported by laboratory tests and MC simulations. This issue was not discovered until the LHC beam turned on despite many test runs for the CMS EMCal prototypes at many facilities. One of our goals is to make sure that we run our EIC detector prototype under the RHIC environment as well.

SiPMs are commonly believed being insensitive to NCE (Nuclear Counting Effect). However, the same was also believed to be true for the thin APDs developed for CMS. To our knowledge, there were no direct attempts to observe anomalous signals in SiPMs in real experimental conditions. As a first step to test EIC EMCals in real experimental conditions we propose to place two EMCal prototypes at the East side at the STAR IP during Run16.

One will be a reworked, old EMCal prototype equipped with readout from both ends. On one side we will use the same SiPM readout we used in the test beam. The other side of the detector will use readout with a single PMT. A high tower trigger will be constructed from SiPM signals from the central four towers in the

matrix. Direct correlations between SiPMs signals and PMTs will unambiguously determine the presence of anomalous signals, if any.

The second prototype will be optimized for APD readout. We will use green 3HF fibers instead of blue SCSF78 to better match APD sensitivity and slow down the light collection scheme. (3HF fibers are few ns slower than blue SCSF78). Again, we will read out this prototype from both ends (PMT from one end of the fibers and APDs from the other) and will have a high tower trigger made from APDs signals. We expect to observe the anomalous signals seen by CMS in this prototype.

Both prototypes will have a monitoring system, and setup will be augmented with He3 counters and CERN RadMon devices to measure neutron fluxes. A complete MC model of the STAR IP and environment and an accurate prediction of the neutron fluxes measured in 2013 with He3 counters are necessary requirements for such tests, i.e., we hope to have well-controlled experiment.

A readout based on APDs may be required in the final EIC detector design for the portion of the detector close to the beam pipe. This is the second reason to prepare an additional prototype with readout based on APDs. The radiation hardness of the SiPMs is under investigation and results are reported by the BNL group of the calorimeter consortium.

For future developments, probably, the best time window to build large scale (256 ch. EM forward calorimeter and 16 ch. HAD calorimeter (with parts utilized from STAR forward prototype) is the long RHIC shutdown in 2018. We have discussed with the STAR management and operations team about the possibility of using the East side of the STAR detector for these tests and the response was very supportive.

### **Additional information:**

We experienced abnormal hardships during the latest test run at FNAL. All four CAMAC crates obtained from the FNAL PREP had different problems, which held us from data-taking for one day, until we finally borrowed a working crate from the MTBF group (we had to check all our electronics boards one-by-one prior to that, due to suspicions that one of them was overloading the crates- however, all were found to be perfectly functional). In addition we lost more than a day trying to tune the beam line due to uncertainties with the beam conditions. Discrepancies in beam resolution were noted between our own measurements ( $10\%/\sqrt{E}$ ) in 2014 using our previous prototype and  $5\%/\sqrt{E}$  using an older PbGl calorimeter) and a 'new standard' MTBF PbGl calorimeter installed in the beam line by MINERVA. After consultation with the accelerator physicist and MTBF coordinator we managed to put in the 'old' PbGl calorimeter we used in 2014 and within three hours we measured the normal  $5\%/\sqrt{E}$ , that cleared all uncertainties with respect to beam conditions (and killed the hope that our new detector worked as expected). This is not the last test beam the EIC calorimeter consortium will perform and there is clear need of a good standard calorimeter of our own, which will make future test runs more efficient. There are also limitations with small area scintillation hodoscope used in the past test runs. We think that we will need to invest in 'infrastructure' to make test beams more productive and less stressful. In this year's proposal, we request a small amount of funds to build a new scintillator hodoscope, which will cover an  $8 \times 8 \text{ cm}^2$  area, sufficient for the FNAL test beam, which we will also share with other calorimeter consortium groups.

## Manpower

Personnel supported through R&D funds during past year:

M. Sergeeva (UCLA, undergraduate)

A. Ruckel (UCLA, undergraduate)

K. Landry (UCLA, graduate student)

N. Shah (UCLA, postdoc 1 month)

S. Yang (UCLA, visiting scholar from Fudan University, China.)

Prof. H. Z. Huang and O. Tsai supervised UCLA personnel. O. Tsai spent about 30% of his time working on the EIC R&D project.

Participants of the 2015 Test Run at FNAL:

Prof. C. Gagliardi (TAMY), C. Dilks (PSU, graduate student), A. Kiselev (BNL), J. Dunkelberger (UCLA, graduate student), M. Sergeeva (UCLA, now accepted to UCLA graduate school), O. Tsai (UCLA).

## Budget Request for FY2016

Hamamatsu H6559 PMT assemblies (2)	\$2.5k
Kuraray 3HF and SCSF78 fibers	\$10k
Tungsten Powder	\$7k
Hamamatsu S8664-1010 APDs	\$15k
Hamamatsu MPPC	\$2.8k
Supplies (Epoxy, etc.)	\$5k
Machine Shop (26% overhead included)	\$12.6k
Travel (FNAL test run, EIC meetings)(26% overhead included)	\$18.9k
Support for undergraduate students (26% overhead included)	\$12.6k
SENSL SiPMs for new Sc. Hodoscope	\$3k
CMC080 qADC (2 x 16 channels)	\$8k
FEEs for APD readout (components only)	\$3k
PS300 Power Supply (APD bias)	\$1.4k
Total Direct	\$92.7k
Total	\$101.8k

## External Funding

STAR has a R&D project for the forward detector upgrade. The IU group will develop the FEE board for APD readout and the engineering support will be covered by the STAR fund.

## Publications:

1. Journal of Physics: Conference Series 404 (2012) 012023 O. D. Tsai, et.al. 'Results of R&D on a new construction technique for W/ScFi Calorimeters' Talk at CALOR 2012.
2. Journal of Physics: Conference Series 587(2015) 01205 O. D. Tsai, et.al.

‘Development of a forward calorimeter system for the STAR experiment’

Both test beam results for the STAR forward calorimeter system and EIC barrel EMcal were presented in a single talk at CALOR 2014.

3. NIM A 756(2014) 68-72 Y. Fisyak et.al.’ Thermal neutron flux measurements in the STAR experimental hall’.

**Subproject Name: EIC Calorimeter Development at BNL**  
**Project Leader: C. Woody**

## **Abstract**

R&D at BNL on calorimeter development for EIC was focused in two main areas. The first was developing techniques for producing tungsten scintillating fiber SPACAL modules which would be used in the central barrel calorimeter of an EIC detector, and the second was to study radiation damage in SiPMs. We also had a third area of R&D, which was studying scintillating crystals for the forward calorimeter in the electron going direction at EIC, but that is covered in a separate part of this report. The work on producing SPACAL modules involved efforts not only at BNL but also at a private company and at other institutions. We initially focused on building modules similar to the ones produced at UCLA that showed excellent performance in test beam measurements carried out in 2014. We first concentrated on trying to reproduce building those modules at other places, and will then extend that technology to enable construction of fully projective modules that would be required by the sPHENIX experiment at RHIC. We also continued our investigation of radiation damage in SiPMs with new measurements at the Low Energy Neutron Source (LENS) at Indiana University where devices were exposed to very high doses of neutrons to see where permanent damage resulting in loss of photon detection efficiency can occur. In addition, we carried out more measurements at RHIC in the PHENIX IR to expose devices to the mixture of radiation that occurs in hadron and heavy ion collisions, which included a special study on the effects of thermal neutrons as requested by the Committee at the last meeting.

## Past

### What was planned for this period?

We planned to produce a number of tungsten scintillating fiber SPACAL modules, essentially identical to the ones produced at UCLA, at several other institutions, and at Tungsten Heavy Powder (THP), which is the company that supplies the raw tungsten powder for producing all of our modules. The goal was to expand the expertise in producing these modules in order to eventually be able to produce the required number of modules for a central barrel electromagnetic calorimeter for EIC either in industry or at one or more university facilities. We succeeded in doing this at BNL, THP and at the University of Illinois at Urbana Champagne (UIUC), which is one of our collaborating institutions on sPHENIX. In addition, new modules were produced at UCLA using an improved and more efficient construction technique. We also planned to build the first fully projective modules, as would be used in sPHENIX, using a new modified technique. However, this required a significant amount of design and development for the tooling, parts and assembly procedure that will be used for this procedure.

We also planned to do more radiation studies on SiPMs. We carried out a test of several devices at the Low Energy Neutron Source (LENS) at Indiana University (with the help of our colleagues from STAR) and characterized devices that had been exposed up to doses of  $10^{13}$  n/cm<sup>2</sup>. We also planned to test a number of SiPMs in the PHENIX IR at RHIC under actual running conditions, including several devices that were shielded from thermal neutrons in order to separate out the possible effects of thermal neutron damage and damage due to other types of radiation.

### What was achieved?

#### *SPACAL module production*

We decided on a standard design for producing modules at each of the various participating institutions, which is the same design as the semi-projective modules that were tested by the UCLA group in the test beam last year and gave excellent resolution. A drawing of this design is shown in Fig.1.

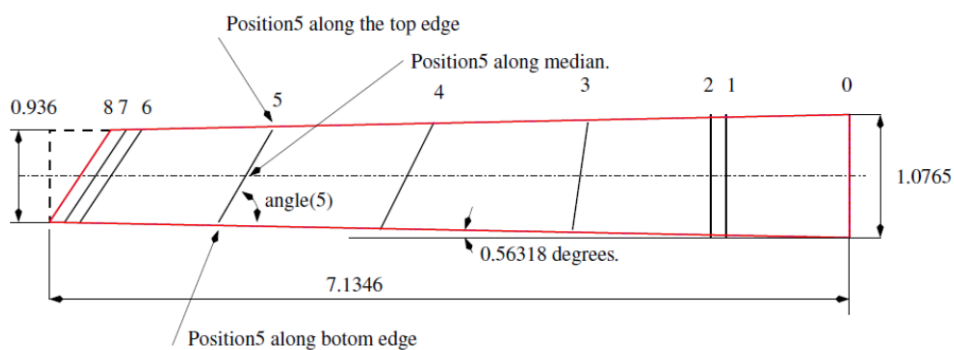


Fig. 1. Drawing of the SPACAL module that was built at each institution participating in the fabrication study. The module design is the same as the ones tested at Fermilab by the UCLA group in 2014.

Figure 2 shows several modules produced at BNL. We developed new tooling for the procedure that was used and made a number of improvements that made the process more efficient. After several attempts, the modules that were produced were of good quality in terms of the uniformity with no obvious bubbles or voids, optical clarity of the fibers, and final density ( $\sim 9.7 \text{ g/cm}^3$ ). However, the construction of these single tapered modules was mainly just a learning exercise in order to be able to produce double tapered (i.e., fully projective) modules in the future as discussed below.

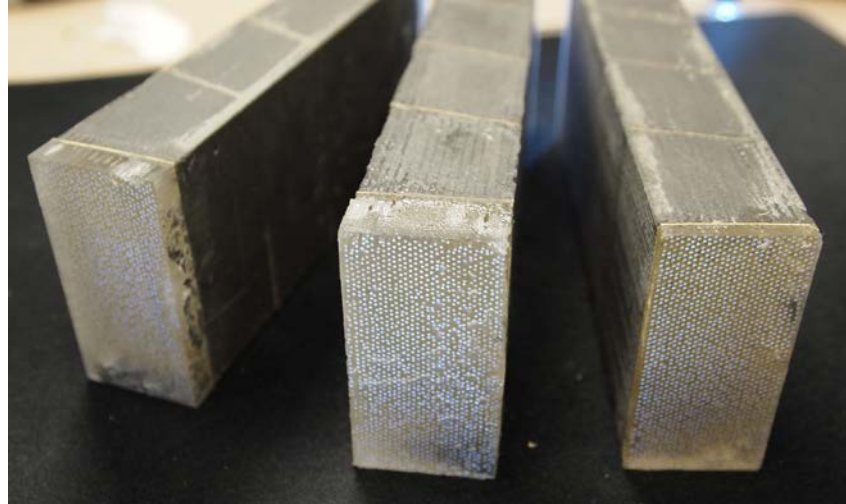


Fig. 2. Single tapered SPACAL modules produced at BNL.

Figure 3 shows two single tapered modules produced at Tungsten Heavy Powder. They used a somewhat different process to produce these modules which they feel is more amenable to being able to mass produce modules in the future. We just received these modules at BNL and the first inspection looks very encouraging. Additional tests will be carried out during the next several weeks. They are still developing their technique and will produce a number of additional modules that will be used in a prototype calorimeter that we plan to test in the test beam at Fermilab next year.

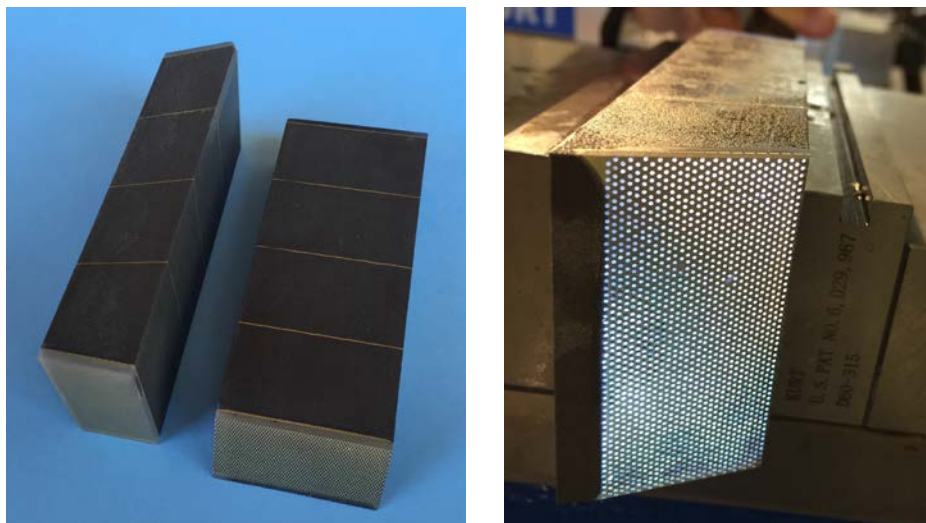


Fig. 3. Single tapered SPACAL modules produced at Tungsten Heavy Powder.

The group at the University of Illinois at Urbana Champagne is also attempting to produce modules. Their effort is just getting under way and they hope to have their first acceptable modules soon. New modules were also produced at UCLA using an improved technique that also increased the efficiency for production and ease of fabrication. Results on this effort will be reported at the upcoming committee meeting

As mentioned above, the production of single tapered modules at BNL was mainly an exercise to learn how to build these modules, with the aim that the techniques developed could be used to produce double tapered modules for the sPHENIX barrel EMCAL. As discussed in our previous report, the idea is to use a set of wire frames that allow the fibers to pass through which can be set at different angles and can achieve a taper in two independent directions. Figure 4 shows again the concept for this procedure. In addition, we will investigate the possibility of using meshes with tapered holes that will allow for the initial stacking of the fibers but can achieve a different spacing when they are positioned within the module. This would allow the construction of trapezoidal shaped modules that have different taper angles in the azimuthal and rapidity directions.

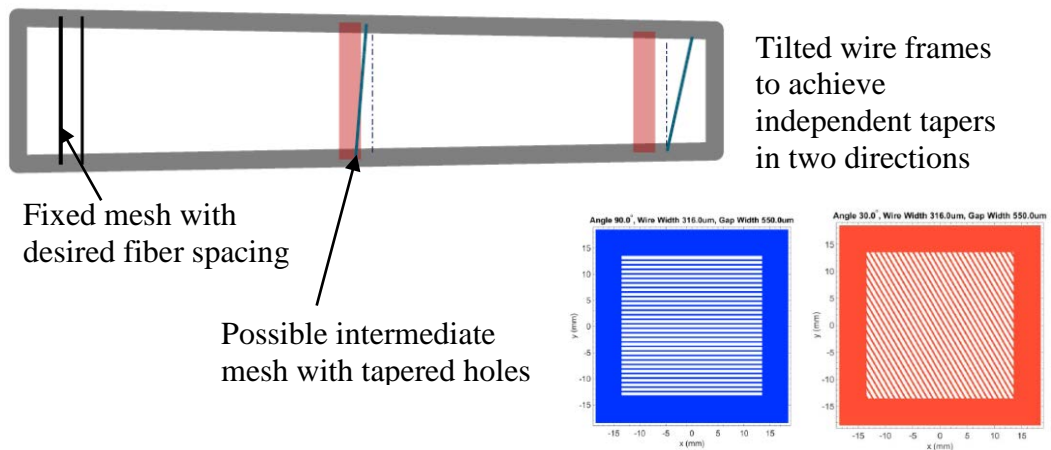


Fig. 4 Conceptual design for producing double tapered modules using two independent wire frames set at different angles and tapered hole meshes.

Due to the precision required, it took a considerable effort to design and produce the drawings that were needed to fabricate all of the parts that will be used for this procedure. These were completed in March and April and all the parts were delivered to BNL by early June. Figure 5 shows a collection of the wire frames and meshes with different wire spacings, hole spacings and thicknesses that will be used for our tests. Fig. 6 shows a drawing of how the fibers and meshes fit together along with a trial assembly of fibers using the tapered hole meshes. However, we still need to design and build the tooling for the mold used to cast the module, which we hope to have completed by the end of July. We plan to do this work at BNL, but our sPHENIX collaborators at UIUC will also attempt to make double tapered modules using this method. In addition, we are developing a full scale engineering design of the entire sPHENIX EMCAL which will incorporate the fully projective modules, along with a detailed Monte Carlo simulation of the calorimeter performance.

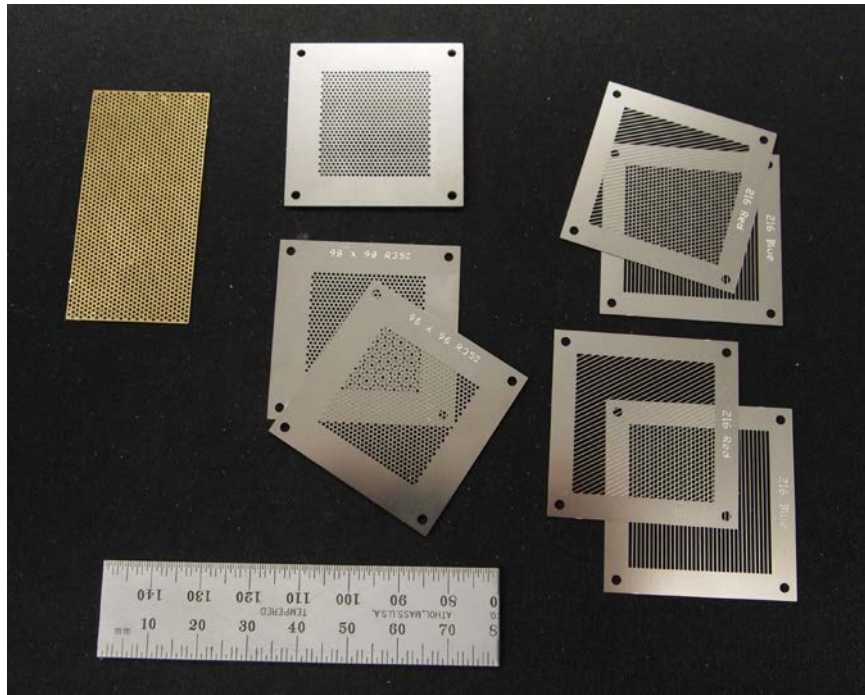


Fig. 5. Wire frames and meshes that will be used to study the construction of double tapered (fully projective) SPACAL modules.

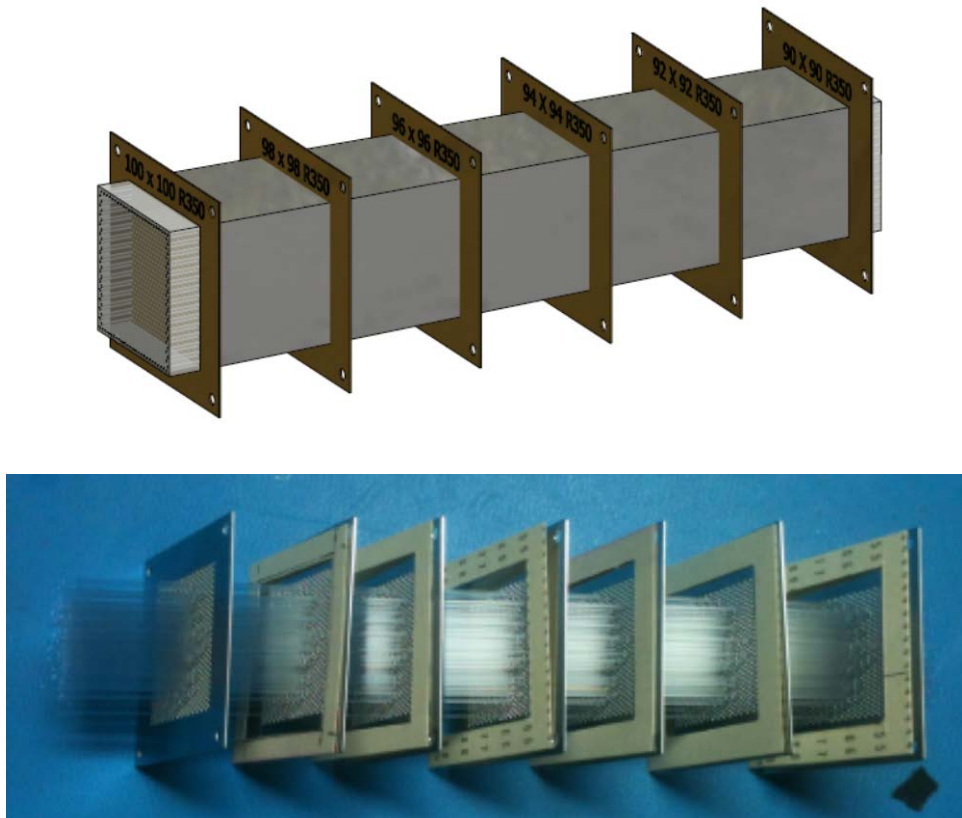


Fig. 6. Top: Design for tapered module assembly; Bottom: Fibers inserted in tapered hole meshes giving the required spacing for a double tapered module.

## Radiation Damage in SiPMs

We exposed a group of SiPMs to high levels of neutron fluence at the Indiana University Low Energy Neutron Source (LENS) in order to measure the effect of high dose levels on the noise and photon detection efficiency (PDE) of these devices. They were characterized before and after irradiation at BNL, and the exposure was carried out with the help of our collaborators from STAR (H.Crawford, L. Bland and G.Visser).

Figure 7 shows a comparison of the dark currents for a group of Hamamatsu S12572-025P SiPMs that were exposed to various levels of neutron fluence. From an initial current  $\sim 100$  nA at the normal operating voltage, the dark current increase by a factor  $\sim 60$  after an exposure of  $10^9$  n/cm<sup>2</sup>. The current continues to grow with increasing exposure up to  $\sim 1$  mA at an integrated dose of  $10^{12}$  -  $10^{13}$  n/cm<sup>2</sup>. This is a very large current for a single device and it could probably not be used with this level of dark current in an actual detector.

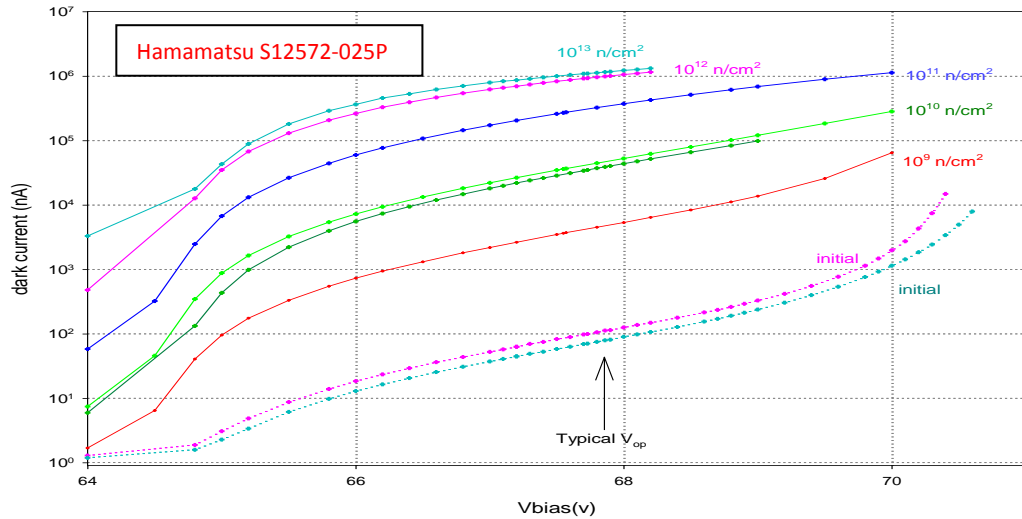


Fig. 7. Increase in noise for a group of Hamamatsu S12572-025P SiPMs exposed to various levels of neutron fluence at the LENS facility.

It should be mentioned that one does not expect neutron doses at the level  $10^{13}$  n/cm<sup>2</sup> at eRHIC or EIC. The actual levels have not yet been estimated (due to the difficulty of doing the calculation), but for comparison, based on measurements of thermal neutrons and a GEANT simulation, STAR estimated that the dose levels reached at STAR during one RHIC run were  $\sim 2 \times 10^{10}$  n/cm<sup>2</sup> at a distance of one meter from the IP. Nevertheless, it appears that one should expect very high levels of dark current for SiPMs in such a high radiation environment. Possible ways of dealing with these effects, such as using devices with more numerous and smaller pixels, as well as cooling the devices, are being explored.

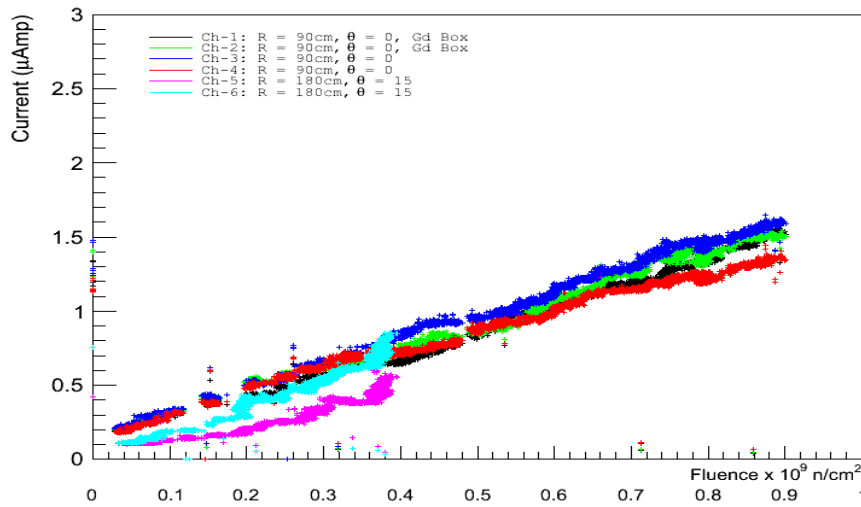


Fig. 8. Hamamatsu S12572-015P SiPMs placed in the PHENIX IR during the current RHIC run. Channels 1&2 were enclosed in a Gd box that absorbed all thermal neutrons. Channels 3&4 were unshielded in the same location. Channels 5&6 were also unshielded and located at the base of the central magnet next to a SPACAL block.

We are also studying a group of SiPMs in the PHENIX IR during the current RHIC run. These measurements are still under way, but some preliminary results are available. Figure 8 shows a set of 6 Hamamatsu S12572-015P SiPMs ( $3 \times 3 \text{ mm}^2$  with  $15 \text{ }\mu\text{m}$  pixels) that were placed in the region of the PHENIX central magnet. Two (Chs 1&2) were placed at a distance of 90 cm from the center of the IP and enclosed in a Gd box that absorbed all thermal neutrons. Two more (Chs 3&4) were unshielded and placed in the same location. Two more (Chs 5&6) were also unshielded and placed at the base of the central magnet adjacent to a SPACAL block in order to study the effect of any spallation neutrons. The neutron fluence was estimated using SiPIN detectors (Radmons obtained from CERN) that are sensitive to a variety of particles, including neutrons.

The devices located 90 cm from the IP have reached a dose level of  $\sim 0.9 \times 10^9 \text{ n/cm}^2$ , while the ones located at the base of the central magnet have reached a level  $\sim 0.4 \times 10^9 \text{ n/cm}^2$ . The increase in dark current as a function of dose seems to lie along the same trajectory for all the devices. We see no difference between the SiPMs that are inside the Gd box or next to the SPACAL block compared to the ones that are not shielded. We therefore conclude that there is no effect of thermal neutrons or spallation neutrons on the increase in the dark current, and it is therefore most likely that it is the neutrons in the MeV range that are causing the damage. We also contacted Hamamatsu and asked them whether boron doping in their SiPMs could possibly result in higher damage due to thermal neutrons being captured compared to other silicon detectors. They claimed they did not believe this would be the case, and our results seem to confirm this claim.

We also have several additional SiPMs with  $10 \text{ }\mu\text{m}$ ,  $15 \text{ }\mu\text{m}$  and  $25 \text{ }\mu\text{m}$  pixel sizes that are connected to scintillators in the PHENIX IR which we are using

to monitor the dark current and light detection efficiency. In addition, we installed again the He-3 thermal neutron detector in the IR and are measuring the neutron fluence the area which will be used as a cross calibration of the Radmons. Results from these measurements will be presented at the committee meeting.

### **What was not achieved, why not, and what will be done to correct?**

We did not begin to construct double tapered fully projective modules due to the delay in designing the wire frames and tapered hole meshes and producing the drawings that were required for ordering the parts. This was a more tedious and lengthy process than we had anticipated, but all the parts were ordered and have now been delivered to BNL. We now need to design the tooling, molds and assembly fixtures that we will be used to try and build the modules, which we hope to have completed by the end of July. We hope to have results on producing the first double tapered modules by the next committee meeting.

We also did not get all the modules from THP that we hoped to have by this time. That process also took longer than expected, but the first modules have now been produced and delivered to BNL. The initial inspection of these modules looks very encouraging and we will now perform more tests on them to see if they meet our specifications. If they do, we will ask THP to produce more modules using the methods they have developed. However, we may change the design slightly for the additional modules in order that they are more suitable to be used in the prototype detector we are planning to test at Fermilab next year.

Our tests of SiPMs in the PHENIX IR at RHIC are still ongoing, and we plan to analyze the data from those tests over the summer. We will have measurements on the increase of the dark currents of many devices with various pixel sizes, as well as a measure of any effect on the light detection efficiency. We will also have a better calibration of the neutron fluence in the PHENIX IR using the He-3 detector.

## **Future**

*What is planned for the next funding cycle and beyond? How, if at all, is this planning different from the original plan?*

Our main emphasis for the next funding cycle will be to attempt to build fully projective modules using a procedure that could lead to cost effective mass production of the modules needed for a central barrel calorimeter for EIC. The focus will be specifically on the sPHENIX barrel EMCAL design, but the techniques developed should be applicable to any SPACAL calorimeter (projective or non-projective) for EIC. The R&D effort on developing the double tapered modules will take place mainly at BNL and UIUC. THP will focus on improving their procedure for producing single tapered modules and developing the techniques needed for mass production. We hope that they will be able to produce enough modules to build an 8x8 array of single projective towers by the fall of this year. We will then use these modules to build a prototype detector which we will test at Fermilab next year. In parallel, once we have developed the procedure for producing the double tapered modules,

we will transfer this technology to THP and have them adapt it to their mass production technique. We will then ask them to produce a second 8x8 array of towers with a fully projective geometry representative of the maximum rapidity coverage ( $\eta \sim 1$ ) for sPHENIX. These modules will be used to construct a second prototype calorimeter that will be tested at Fermilab later next year.

We will also continue our studies on radiation damage in SiPMs. We plan to carry out more studies on the Hamamatsu devices (in particular those with 10  $\mu\text{m}$  and 15  $\mu\text{m}$  pixel size) as well as devices from other manufacturers. This will involve additional measurements using the 14 MeV neutron generator at the Solid State Radiation Facility at BNL as well as possible additional tests at other facilities, such as LENS or Los Alamos. It should be noted that it would be of great benefit to our program to study radiation damage in SiPMs to be able to use our own NSRL Facility here at BNL to study proton damage in these devices, but the cost is simply too high (\$5k/hr). We had to abandon such a test in the spring of this year for this very reason.

It appears that the increase in dark current in SiPMs with neutron dose is unavoidable a certain level, so we will have to devise ways of dealing with it in any detector that will be used in an experiment where the radiation levels are high. We will therefore start to develop ways of coping with this effect in the calibration and control system for the SiPMs. We know the voltage biasing system must provide a way to compensate for the steep dependence of the SiPM gain with temperature, so it should now also include a way to compensate for the increase in leakage current and its effect on the bias voltage with radiation exposure.

The radiation effects can be minimized by using devices with smaller pixel size and by cooling. The new Hamamatsu devices with 15  $\mu\text{m}$  pixel size have essentially the same PDE (25%) as their previous version with 25  $\mu\text{m}$  pixels, so there is a clear advantage in using them in a high radiation environment (in addition, they have 40K pixels vs 14.4K pixels and therefore provide greater dynamic range). The 10  $\mu\text{m}$  devices have a factor of 2.5 lower PDE (10%), but have shown lower increases in dark current in some tests. We will perform tests in the lab to characterize various devices at low temperature before and after radiation and determine how the dark current can be minimized with a hopefully moderate lowering of the temperature. Once the optimal operating conditions have been determined, we will implement this into the design of the calorimeter and its readout electronics. We hope to be able to test these features in our beam tests at Fermilab next year.

All of the above activities are within the scope of the original BNL R&D plan for calorimeter development. The main change is that there is now a focus on the barrel EMCAL design for sPHENIX.

*What are critical issues?*

The two main critical issues for the next R&D period are: 1) to demonstrate that it is possible to build fully projective calorimeter modules in a cost effective way, and 2) to start to develop a control and readout system that can

cope with the expected increase in dark current of the SiPMs in a high radiation environment.

Being able to produce fully projective calorimeter modules is an important requirement for the sPHENIX barrel EMCAL, since it affects the ability to achieve good electron hadron separation at larger rapidities in high multiplicity heavy ion collisions. The projectivity requirement is not so important for an EIC detector due to the much lower multiplicity, but since the sPHENIX calorimeter will be used as a Day-1 detector for EIC, the same calorimeter must satisfy the requirements for both experiments. It should be noted that the energy resolution requirement for sPHENIX is somewhat less stringent than for EIC ( $\sim 15\%/\sqrt{E}$  vs  $10\text{-}12\%/\sqrt{E}$ ), but the sPHENIX calorimeter is also being designed in order to provide the better resolution required for EIC.

The design of a cooled and stabilized temperature control system for the SiPMs is critical in order to maintain their gain stability. We have already developed a bias control system for the SiPMs which measures the temperature of individual groups of SiPMs (4 per readout tower) and adjusts the bias voltage to maintain a constant gain. However, by limiting the temperature variations to a small range, the required adjustments to the bias voltage are minimized. With the expected increase in dark current due to radiation damage, it will be highly beneficial to maintain the operating temperature below room temperature in order to minimize the effect of the increased noise. We have not yet determined what temperature this should be, but we hope that our next set of measurements will help us determine this.

*Additional information:*

## **Manpower**

*Include a list of the existing manpower and what approximate fraction each has spent on the project. If students and/or postdocs were funded through the R&D, please state where they were located and who supervised their work.*

The effort at BNL on the projective modules for the sPHENIX barrel EMCAL includes one Senior Scientist (0.5 FTE), one Assistant Scientist (0.2 FTE), one Physics Associate (0.8 FTE), one Mechanical Engineer (0.1 FTE), one Designer (0.1 FTE) and one Technician (0.3 FTE). These personnel are all paid by the BNL Physics Department. The R&D effort on projective modules at UIUC includes one Assistant Professor (0.1 FTE), one Postdoc (0.75 FTE) and two technicians (0.25 FTE), all paid by UIUC. The overall effort at BNL on the readout electronics and control system for the SiPMs for sPHENIX includes one Physics Associate (0.8 FTE), one Electrical Engineer (0.9 FTE) and one Technician (0.5 FTE), all paid by the BNL Physics Department. However, the fraction of their time devoted to work on SiPM radiation damage and its effect on the electronics and control system is  $\sim 5\%$ .

## **External Funding**

*Describe what external funding was obtained, if any. The report must clarify what has been accomplished with the EIC R&D funds and what came as a contribution from potential collaborators.*

The R&D on the projective calorimeter modules is supported mainly from PHENIX R&D funds. However, the work on studying radiation damage in SiPMs is not directly funded by PHENIX, and is also applicable to other EIC detectors that will use SiPMs.

## **Publications**

*Please provide a list of publications coming out of the R&D effort.*

This R&D was also a part of the R&D for the central barrel EMCAL for sPHENIX and is included in the following publication.

“Design Studies of the Calorimeter Systems for the sPHENIX Experiment at RHIC and Future Upgrade Plans”, C. Woody and E. Kistenev, Proceedings of CALOR 2014 International Conference on Calorimetry in High Energy Physics, J. Phys. Conf. Ser. Vol. 587(1) 011001 (2015).

**Sub Project: Crystal Calorimeter Development based on PbWO<sub>4</sub>**  
**Project Leader: T. Horn**

**Overview**

An important requirement for the EIC endcap electromagnetic calorimeter is high-resolution in the electron going direction in order to measure the energy of the scattered electron with high precision. The best detector resolution at small angles, where the tracking resolution is poor, could be achieved by a *high-resolution crystal inner part*. As described in the EIC WP this *inner calorimeter* should provide angular resolution to at least 1 degree to distinguish between clusters, have an energy resolution  $\sim \text{few } \%/ \sqrt{E}$  for measurements of the cluster energy, and withstand radiation to at least 1 degree with respect to the beam line. An *inner calorimeter* based on PbWO<sub>4</sub> crystals would be an optimal solution due to its small Moliere radius. The main goal addressed by this R&D effort is to identify what would need to be done to be able to build a PbWO<sub>4</sub>-based endcap calorimeter for the EIC exploring the limits of PbWO<sub>4</sub> quality. In the past funding period we focused on setting up infrastructure for crystal testing, understanding systematic effects in the crystal testing method' and starting to develop methods to characterize radiation damage effects on crystals. In this report we also show the results of tests with the first full-size PWO crystal produced at Crytur. Our main goals for the upcoming period include the completion of infrastructure for crystal testing, a conclusion on what is possible in terms of crystal quality of SIC crystals and the first evaluation of crystal-to-crystal variations of Crytur produced crystals . We are also planning to construct a prototype, which would allow us to study the crystals in test beam and measure the actual energy and position resolution that we could achieve with them. These measurements would provide important information on crystal specifications.

**Past**

**What was planned for this period?**

The main goals for this project in this time period were:

- Set up the infrastructure for crystal testing.
- Understand systematic effects in the crystal testing method
- Start developing methods to characterize radiation damage effects on crystals
- Plan meetings for 2015 to exchange information on crystal testing.

**What was achieved?**

**Infrastructure for crystal testing at the universities**

To test the crystal performance the university lab infrastructure at IPN-Orsay and CUA has been optimized for such tests. The group (G. Charles and C. Munoz-

Camacho) at IPN-Orsay has started setting up the necessary infrastructure to perform crystal quality tests. Using crystals originally manufactured by BTCP (Russia), borrowed from the University of Giessen, we have performed transmittance measurements, both longitudinal and transverse to the crystal axis.

We have used a Varian Cary 5000 spectrometer (Fig. 1, left) currently available on Campus at the Institute of Molecular Chemistry and Materials of Orsay (ICMMO). This spectrometer can take absorption measurements along and across the crystals with a 1 nm wavelength resolution between 200 and 800 nm. Collimators are installed in front of the beam source in order to produce a clean beam spot. Typically, 4 absorption spectra were measured: three of them transverse to the block at positions shown in Fig 1 (right) and one longitudinal. The spectrometer is calibrated each time a crystal is changed or moved.

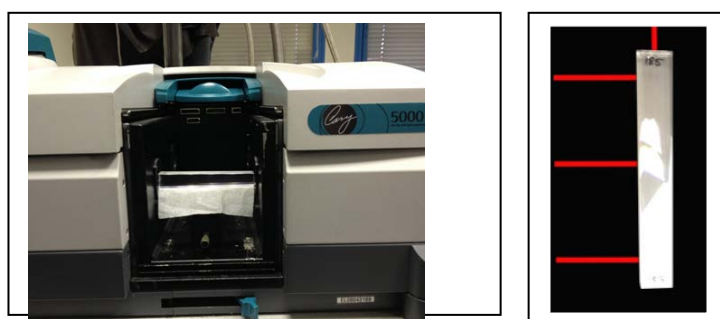


**Fig. 1:** Varian Cary 5000 spectrophotometer with a crystal ready to be tested (left). The approximate positions and directions of the beam used to measure the crystal absorption are shown in red (right).

Transmittance results obtained for a sample crystal are shown in Fig. 2, for all four positions and as a function of the incident beam wavelength. Transmittance starts around 350 nm and reaches values close to 90% at higher wavelengths.

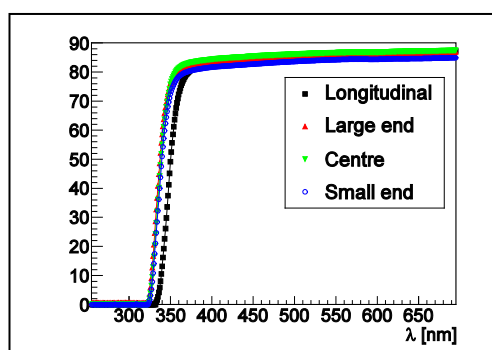


**Fig 2:** Crystal transmittance (%) as a function of the wavelength for different incident beam positions (3 transverse to the crystal, and one longitudinal).

The sample compartment of the Varian Cary 5000 spectrometer only allows fitting blocks up to 15 cm long. In order to perform measurements on longer crystals, IPN-

Orsay has ordered a fiber-based spectrometer that will allow a more versatile configuration for measurements. Its delivery is expected end of June 2015.

Additionally, a setup to measure the crystal light yield is being implemented, using a radioactive source and a calibrated PMT. Initially, the setup is being tested with cosmic rays in order to get the data acquisition and detector systems ready. Two scintillators in coincidence are used to trigger cosmic events through the PbWO block placed between them. A PMT is attached to the block and its gain was calibrated using the single photo-electron peak. Fig. 3 shows the results of the PMT calibration. The cosmic spectrum in the block is shown in Fig. 4 where we can see that the cosmic signal is well separated from the pedestal. The mean value of the Gaussian fit is 182 ADC channels with a pedestal at channel 72. Using the data below for our setup, this yields 117 photons per MeV at room temperature, which is very close to values measured for these crystals by other groups.

- Average thickness of the crystal: 2.1 cm
- ADC sensitivity: 0.25 pC/channel
- PMT gain:  $4.1 \cdot 10^5$
- PMT QE: 25%
- Light collection efficiency: 70%

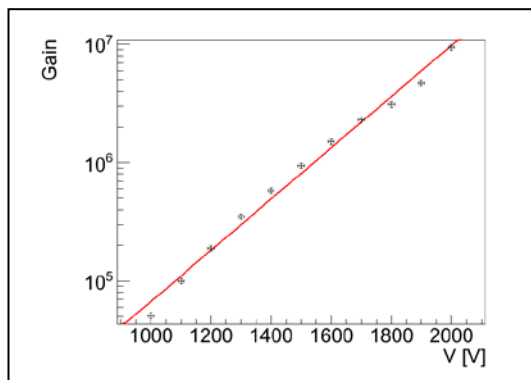


**Fig 3:** Calibration of the PMT used for the light yield measurement. The single photo-electron peak was used in order to calibrate its gain. The red line is an exponential fit to the gain as a function of the PMT voltage.

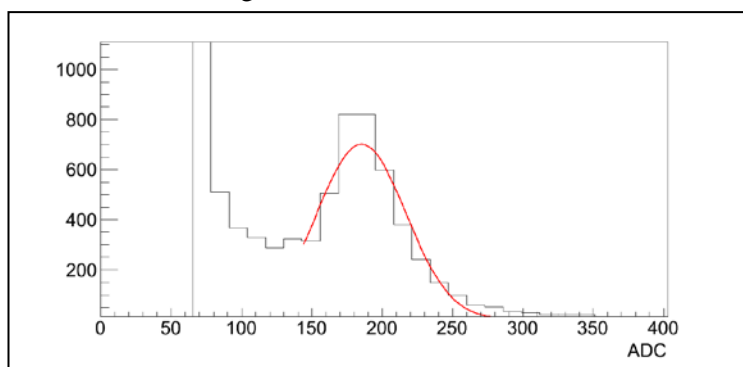


**Fig 4:** Cosmic ray spectrum in one PbWO block. The minimum ionizing peak is clearly visible and can be used to estimate the light yield at room temperature.

The group at CUA (M. Carmignotto, I. Sapkota, A. Mkrtychyan, and T. Horn) has access to a Perkin-Elmer Lambda 750 photo-spectrometer through the Vitreous State Laboratory on campus. The spectrometer allows for measurements of the transmittance and absorption between wavelengths of 200 to 900 nm with 1 nm resolution. The dimensions of the spectrometer compartment accommodate measurements in the longitudinal direction of crystals of lengths up to 20 cm. However, the spectrometer compartment is optimized for characterizing 1-cm long liquid glass samples and had to be modified for measuring the lateral (transverse) characteristics of 20-cm long crystal samples. The modified compartment will be equipped with a horizontal positioning slide and a programmable stepper motor. A photograph and a drawing of the stepper motor Xslide assembly are shown in Fig. 5 (middle, right). The assembly is arranged at an angle of about 30 degrees to avoid interference with the reference beam and the crystal itself. Stepper motor XSlide assemblies are available from several vendors, e.g., Velmex and Parker. The latter has been used by the materials science groups of the Vitreous State Laboratory for the last ten years, while products from the former have been used by the nuclear physics group at CUA. Due to the constraints imposed by the spectrometer compartment we chose the Velmex positioning device depicted in the Fig 5 (middle). An example of the transmittance measurement results is shown in Figure 6 (left).



**Figure 5:** (left) the Perkin Elmer spectrometer at CUA; (middle) Velmex positioning device; (right) schematic of the positioning device and crystal in the spectrometer compartment.

For the calibration of the setup we have been using crystals originally manufactured by BTCP (Russia), borrowed from the University of Giessen and a small crystal sample from SIC borrowed from the Vitreous State Laboratory. Initial results of these transmittance measurements are shown in Figure 6 (middle, right) along with a setup to measure the crystal light yield that is being constructed at CUA. The light yield setup consists of a Na-22 source, a calibrated Hamamatsu R4125 PMT, a collimator, a scintillator to provide triggering, and an ADC-based readout. The system has been tested with cosmic rays and initial measurements with the source have been carried out. The crystal light output is sensitive to temperature. We are thus also investigating options for controlling the temperature of our setup. We expect to have completed the infrastructure setup before the end of FY 2015.

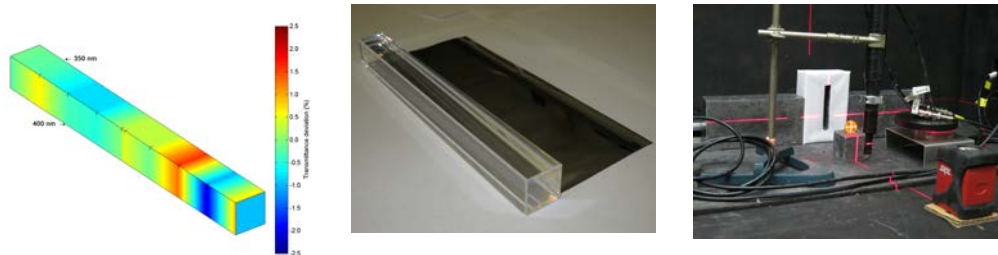


**Figure 6:** (left) transmittance difference for two wavelengths (350 and 400 nm), i.e., how much the light transmittance deviates from the mean transmittance along the crystal along the top and side surfaces; (middle) PWO crystal before wrapping in enhanced specular reflector for light yield tests (right) Setup for initial light yield tests with a Na-22 source.

## Initial Studies of recently produced SIC crystals

### *Transmittance measurements*

One of the currently most representative sets of PWO crystals manufactured by SIC has been measured for optical properties at JLab. The data were taken with a setup consisting of a halogen lamp, integrating sphere, holder table for the crystals and optics. The reproducibility of the transmittance measurements with this setup is on the order of a few percent dominated by uncertainties in positioning the crystal. The longitudinal transmittance results for the 10 crystals produced by SIC in spring 2014 and 5 crystals produced in December 2014 are shown in Fig. 7. The longitudinal transmittance varies between 60% and 70% for most crystals at a wavelength of 420 nm. One of the crystals shows a completely different behavior above 480 nm compared to the other crystals. The transmittance in the transverse direction (2 cm thickness) was measured at several distances ranging between 5 and 55 mm from the face of the crystal.

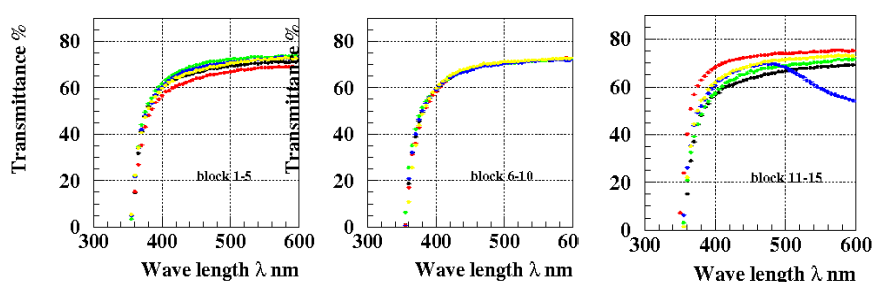


**Figure 7:** (left, middle, right) longitudinal transmittance of PWO crystals produced by SIC in 2014. Crystals #1-#10 were produced in spring and crystals #11-15 were produced in December 2014. The yellow curves in the figures denote crystal #5, 10, and 15. The red curves denote crystal #2, 7, and 12. The black curves denote crystal #1, 6, and 11. The green curves denote crystal #3, 8, and 13. The blue curves denote crystal #4, 9, and 14.

The crystal transmittance seems consistent with the CMS quality standards presented in Table 1 of our January 2015 progress report and is relatively uniform along the crystals. However, there is a variation from crystal to crystal on the order of

20%. The transverse transmittance of one of the crystals is significantly lower than that of the other crystals. Evaluation of the variation from crystal to crystal and determining what is acceptable for the EIC inner endcap calorimeter is one of the main goals of this R&D project.

### *Studies of radiation damage effects with electron beam*

To study crystal radiation damage effects we carried out irradiation tests with electron beams in February 2015 at the Idaho Accelerator Facility, which features a 20 MeV electron beam with 100 Hz repetition rate, with  $I_{\text{peak}}=111$  mA (per pulse) and 100 ns pulse width. The beam is roughly 1 mm in diameter and exits through (1/1000)-in thick Ti window, a  $x/X_0 = 7.1 \cdot 10^{-4}$  radiation length. Beam position and profile are measured by shooting a glass plate. Scanning the plates and fitting the intensity distribution provides a quantitative (though approximate) measurement of the position and size of the beam at the location of the plate. The front plate was placed at the position of the PbWO<sub>4</sub> crystal front faces during irradiation that is 10.75 cm from the beam exit window. The rear plate was located at 51.15 cm from the beam exit, and shows the beam profile expansion. The beam profile at the entrance of the PbWO<sub>4</sub> crystals has an approximate size of 0.2-0.3 cm (sigma). This is much smaller than the transverse size of the PbWO<sub>4</sub> crystals, so the distance of the PbWO<sub>4</sub> crystals was increased the second irradiation day to 33 cm from the exit window. This provides a more homogeneous irradiation and heat load on the crystals. A PbWO<sub>4</sub> crystal of mass  $M = 0.6$  kg at the above mentioned beam parameters will receive a dose:

$$D(\text{Gy}) = \frac{111 \cdot 10^{-3} \times 100 \cdot 10^{-9} \cdot 3.2 \cdot 10^{-12} \cdot 100 / 1.61 \cdot 10^{-19}}{0.6} \approx 36 \text{ Gy/sec},$$

or 216 krad/min. Since such radiation dose rate is too high (~13 Mrad/h), our tests were carried out at ~1000 times lower dose rates (~13 krad/h) at a reduced accelerator repetition rate of 0.1 Hz, keeping the beam current per pulse and pulse width unchanged (111 mA and 100 ns). The measured difference of the crystal transmittance before and after irradiation is illustrated in Fig. 8. All transmittance measurements at the Idaho facility were carried out using an OCEAN OPTICS USB4000 device instead of a permanent spectrometer setup. The reproducibility of measurements with this setup ranges from 5% to 15%.

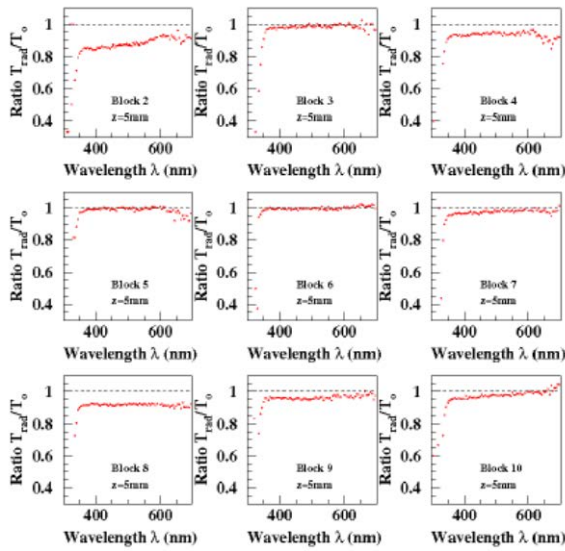


**Figure 8:** The ratio of transmittance before and after irradiation of PbWO<sub>4</sub> crystals after 432 krad accumulated dose at dose rates of 1.3 Mrad/h

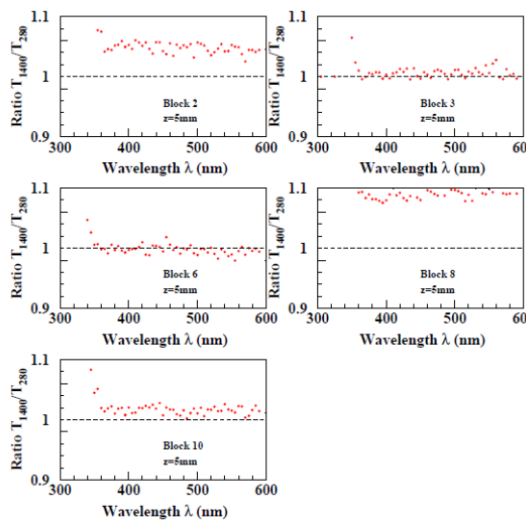


**Figure 9:** Spontaneous recovery of crystals from a 432 krad dose damage, 60 hours after irradiation.

The transmittance of some of crystals changed more than 15% after an accumulated dose of 432 krad (at a dose rate of 1.3 Mrad/h), while others do not seem to show any effects of radiation damage. The change in transmittance for positions far from the front of crystals decreases with the distance. The effect of radiation damage is in part spontaneously recovered after a time period of 60 hours (see Figure 8). Overall the results seem to suggest that the crystals can handle high doses at high dose rates. This is in contrast to earlier crystal test results produced during a similar time frame and presumably under the same conditions.

### *Studies of systematic effects on crystal optical quality*

Understanding the effect of systematic effects on the optical measurements is important for the interpretation of crystal quality. Fig. 8 shows transmittance measurement results before irradiation taken with the OCEAN OPTICS USB4000 device on two different days. Comparison of these measurements gives a qualitative number on the accuracy of the transmission measurements performed before irradiation of the blocks. The systematic difference between these two measurements on average ranges between 5% and 15%. For comparison, the expected intrinsic accuracy of transmittance measurements with photo-spectrometers is <1%. Additional systematic uncertainties in the measurements may result from different setups, e.g., beam vs. source, and may affect the interpretation of not only optical, but also the effect of radiation damage on the crystals.

One of the challenges in irradiation studies with beam is temperature control. Ideally one would control the temperature variation during the irradiation measurement within a few percent. This is difficult to achieve when working with an intense and narrowly focused beams, which give a high and concentrated dose to the crystals, and can even result in heating and thermal damage. As an example, for irradiation at a dose rate of 1.3 Mrad/hr, the temperature near the face of the crystal ramped up at a rate of 0.5 degrees/minute. For irradiation at a dose rate of 2.6 Mrad/hr, a rise of the temperature of more than 2C/minute resulted in severe structural damage to the crystal after 10 minutes. To reach higher doses crystals thus needed to be allowed to cool down between exposures.

Another challenge in this measurement of radiation damage effects is to minimize surface effects. Ideally, one would measure the same spot before and after radiation minimizing surface effects in the path. Care was taken to ensure that this condition was satisfied and the flat distributions in Fig. 8 seem to suggest that our setup satisfied this condition. To minimize the effect of spontaneous recovery on our measurements we carried out the transmittance measurement 10 minutes after irradiation. During these 10 minutes the no special care was taken to minimize ambient light exposure of the crystals. The impact of recovery due to ambient light during this time and systematic uncertainties due to fast recovery components is being investigated.

While we could control many of the systematic effects on the measurement it is important to confirm our results and quantify any setup dependent effects. For instance, it is known that there are strong dose rate dependent effects in crystals and their performance under the extreme conditions of our beam tests may be different than at lower dose rates. In general, lower dose rates are more representative of what one would expect in an experiment. A subset of the ten crystals tested with beam at Idaho is being tested with radioactive sources at Caltech, BNL, and Giessen. These sources will provide a more uniform dose and lower dose rate and comparison of the

results will allow for understanding setup dependent effects in radiation damage studies. The Caltech facility has been used for CMS crystal measurements and Giessen is testing crystals for PANDA EMC. Measurements at Caltech will allow for studying radiation damage effects also comparing to earlier tests of CMS crystals. Caltech has Co-60 (100 rad/hr) and Cs-137 (6000 rad/hr) sources. BNL has a Co-60 source and also a neutron generator. Crystals #5 and #11 were sent to Caltech, crystals #7 and #15 were sent to BNL, and crystals #2, 3, 6, 8, and 9 were sent to Giessen. Crystals #11 and #15 have never been irradiated. The remaining crystals were irradiated in Idaho and subsequently thermally annealed. Initial results of transmittance measurements of crystals #7 and crystal #15 carried out at BNL are shown in Figure 11.

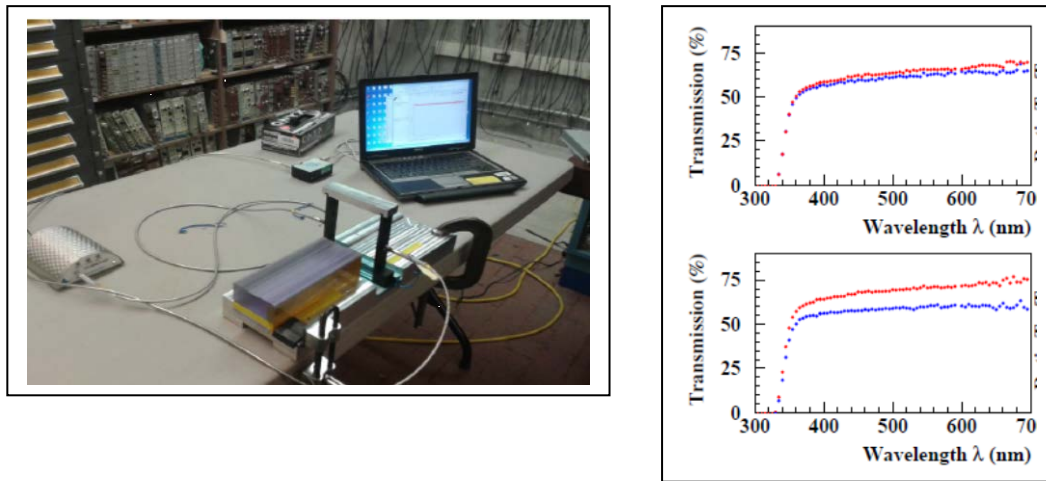


**Figure 10:** (left) OCEAN OPTICS USB4000 portable device for the measurement of crystal transmittance;(right) transverse transmittance at a distance of 5 mm from the crystal face for two crystals taken on two different days before irradiation.

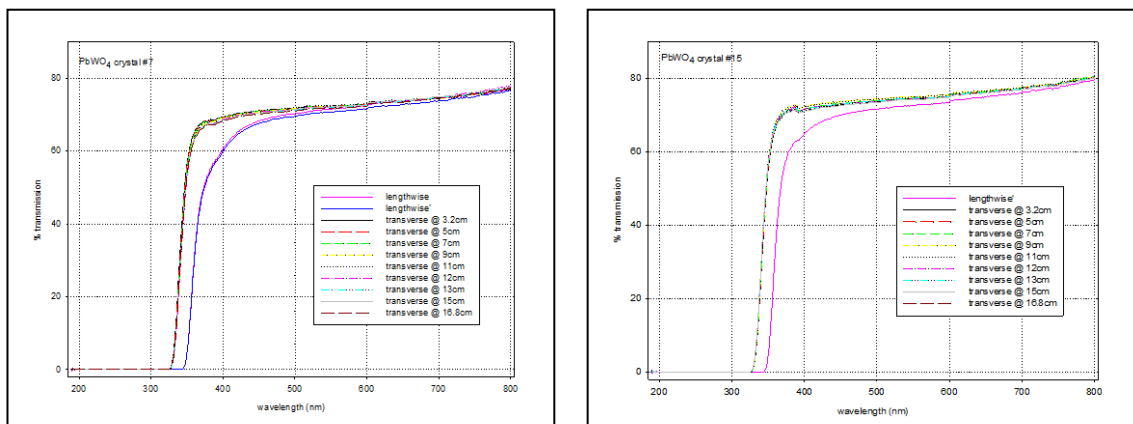


**Figure 11:** (left) transmittance of SIC crystal #7 (left) and crystal #15 (right) as measured in the setup at BNL.

Compared to the measurements at JLab shown in Figure 8 these results show a similar trend, but the magnitude of the longitudinal transmittance of crystal sample #15 is lower by about 5% at ~400 nm. Understanding this difference is part of our ongoing setup dependent systematic effects studies. The variation in transmittance between these two crystals is on the order of 5-7% at 400 nm.

Preliminary results from measurements at Giessen show similar features to those found in the BNL measurement in that the measured values of the transmittance are lower than those shown in Fig. 8 for the JLab measurement. On average the values are lower by 10-15% though for crystal #2 the difference is more than three times as much. It is interesting to note that there seems to be a significant difference in the shape of the distribution between the JLab and Giessen measurements in the region around 400 nm. Preliminary results of the light output of crystal #2 shows a value consistent with CMS standards while no clearly interpretable result could be determined for crystal #3. Preliminary results of the absorption coefficient show that four out of five crystals would pass the crystal specification in Table 1 of our 2015 January progress report. Studies to understand these results and any setup dependent systematic effects are ongoing.

A comparison of CMS average crystal quality to initial test results of transmittance, light output and decay kinetics measurements of crystals #5 and crystal #11 carried out at the Caltech HEP Crystal Laboratory is shown in Figure 12.

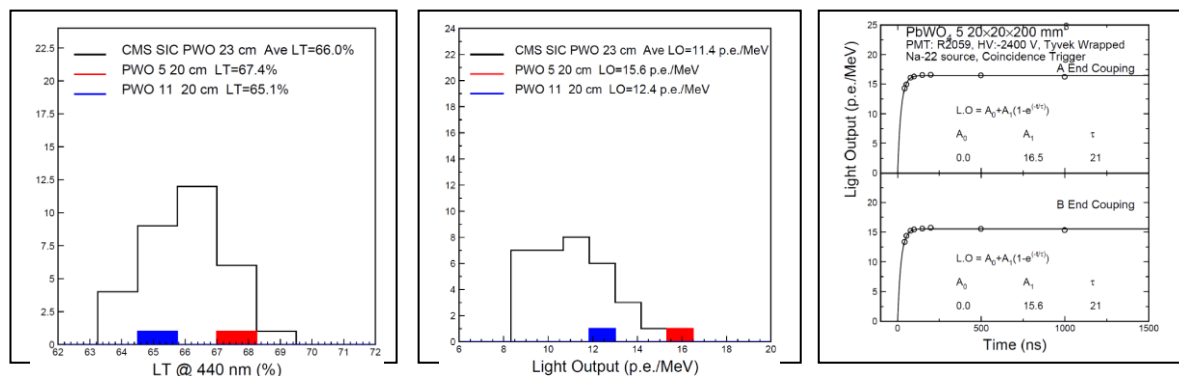


**Figure 12:** (left) transmittance of SIC crystal #5 (red) and crystal #11 (blue) as measured at the Caltech HEP crystal laboratory in comparison with CMS PWO crystal average. (middle) light output of the 2014 crystals compared to CMS crystal average; (right) decay kinetics of the two 2014 crystals in comparison to CMS PWO crystals.

The initial results from the Caltech measurement show a longitudinal transmittance, light output, and decay time of crystals #5 and #11 that is consistent with CMS quality standards as shown in Table 1 of our January 2015 progress report. Detailed analysis shows that crystal #11 has significantly more scattering centers than crystal #5. In comparison to the measurements carried out at JLab shown in Figure 8, the transmittance of the two crystals measured at Caltech is similar in shape, but higher in magnitude. The discrepancy may be caused by the scattering centers, but more detailed investigations to understand systematic effects are ongoing. Irradiation studies to fully understand radiation damage effects will be carried out at Caltech and BNL as well.

## Status of CRYTUR Crystal Production

Since the last progress report update CRYTUR has produced the first 200mm long crystal in rectangular shape (2x2x20cm\*\*3). The crystal was grown making use of pre-production crystals from BTCP as raw material. The crystal has been cut into a rectangular shape, which allows for most efficient investigations of homogeneity, and all surfaces have been polished. The crystal is shown in Figure 13. One can see that the crystal has a longitudinal non-uniformity of macro defects. The results of the first optical and radiation hardness properties have been carried out. The results are shown in Figure 14 compared to the performance of a representative BTCP crystal. The transmittance of the crystal grown at Crytur falls within 8% of the BTCP crystal at 420 nm. The induced absorption coefficient up to 150 Gy, as well as the transmittance at luminescence maximum is consistent with the strict PANDA crystal specifications shown in Table 1 in our January 2015 progress report.

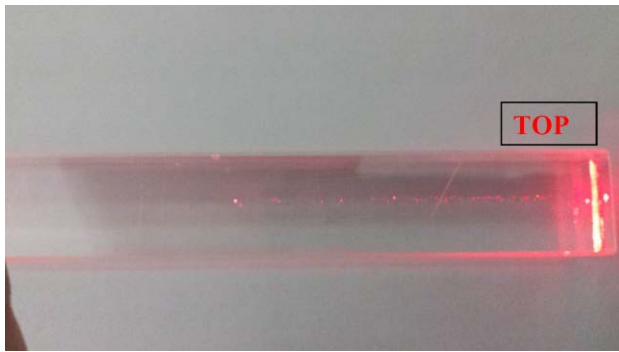


**Figure 13:** First full-size crystal grown at Crytur using pre-production crystals from BTCP as raw material. The crystal shows macro defects in the longitudinal direction.

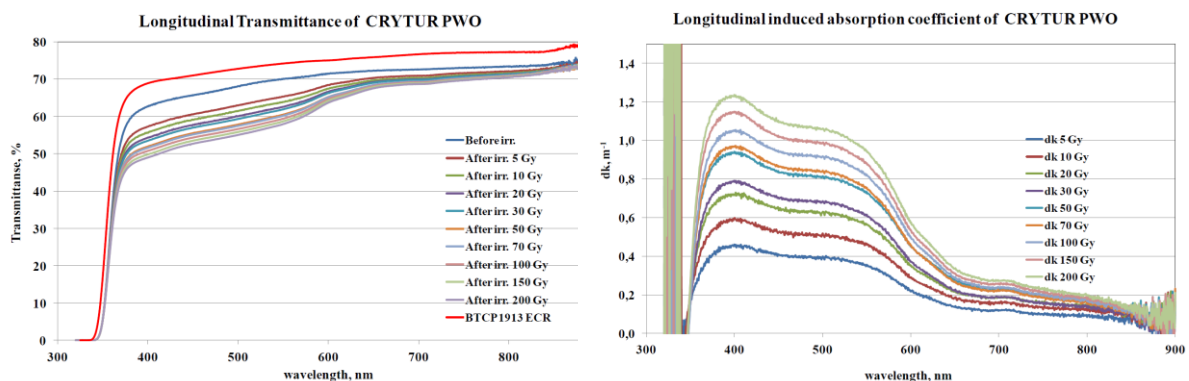


**Figure 14:** (left) longitudinal transmittance of the crystal before and after irradiation; (right) longitudinal induced absorption coefficient.

## **Initial light output tests with SiPMs**

At BNL we have carried out initial tests of readout with SiPMs. A setup was constructed with 4 SiPMs coupled to the same crystal. The SiPMs cover about 10% of the corresponding area of a PMT. Measurements with a Cs-137 source showed an energy deposition of 662 keV, which corresponds to about 1 photoelectron. The small size of the signal complicates these measurements and we are exploring alternative setups with cosmic rays.

## **Meetings in 2015**

To take full advantage of the expertise of all collaborators on this project and also the Giessen group (building the EMC for PANDA), a number of meetings were arranged to exchange knowledge. Carlos Munoz-Camacho is visiting the facilities at Caltech and Rainer Novotny will meet with Carlos Munoz-Camacho, Hamlet Mkrtchyan and Tanja Horn at JLab June 15-17 to provide feedback on the procedures for testing the crystal quality.

## **What was not achieved, why not, and what will be done to correct?**

Initial studies of the 2014 SIC produced crystal properties showed puzzling and inconsistent results with earlier studies of crystals produced in a similar time frame and presumably a similar method. We thus do not yet report our final conclusion on the SIC crystal quality. To address this puzzle we are carrying out detailed systematic checks of our methods with the set of SIC 2014 crystals. We are also planning to analyse a set of crystals produced in 2015. A batch on the order of 30 crystals has been ordered from SIC in spring 2015 and should be available for testing later this summer. The first crystal from Crytur just became available and we do not yet have a complete set of measurements to allow us make a determination on the crystal quality from crystal-to-crystal meets our expectations. The company expects that on the order of 20 crystals will be available in July/August 2015.

## **Future**

### **What is planned for the next funding cycle and beyond? How, if at all, is this planning different from the original plan?**

The planning for the next quarter will generally be as outlined in the proposal. Our main priorities will be to complete the infrastructure for crystal testing, and understand the systematic effects in our crystal testing methods to have consistent results on the various crystals. Figure 15 shows radiation hardness studies of crystals from SIC and the first data on a Crytur produced full-size crystal. Since our last update there has been much progress with improving crystal quality at SIC and tremendous progress at Crytur, which resulted in the production of the first full-size crystal. Over the next reporting we expect to have results on crystal-to-crystal performance variation of Crytur crystals for comparison with additional SIC produced

crystals. These results will be important for understanding what is achievable in terms of requirements on radiation hardness in the current production. This also emphasizes the importance of our R&D efforts to continue developing an alternate supplier with Crytur. The general question whether the EIC could use more relaxed crystal specs, also in terms of variations, is a key question of our ongoing R&D.

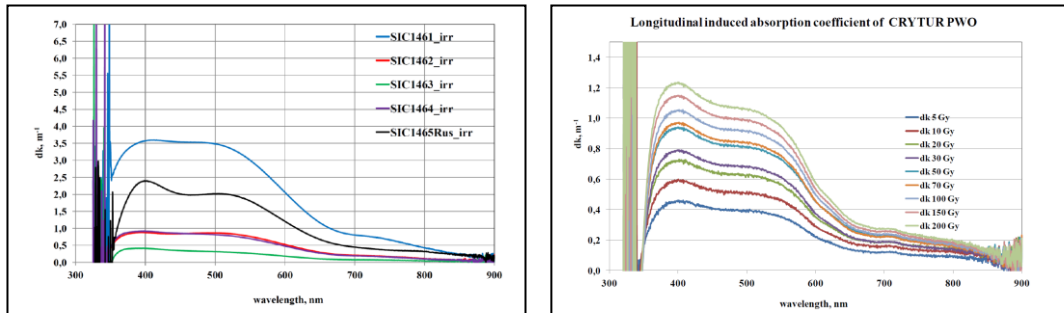


**Figure 15:** Impact of radiation damage in terms of the optical absorption coefficient for (left) 5 PWO crystals from SIC produced in the fall of 2014 and (right) the first full-size Crytur crystal produced in 2015 at different radiation doses. The SIC crystal data show relatively large crystal-to-crystal fluctuations in radiation hardness. Only three out of ten crystals would pass the requirements listed in Table 1.

Assuming that our PbWO<sub>4</sub> crystal studies continue successfully, another main goal for the next period is to build a small prototype detector consisting of a 5x5 matrix of the new improved crystals. This would allow us to study these crystals in test beam and measure the actual energy and position resolution that we could achieve with them. These measurements would provide important information on crystal specifications and their impact on the performance of the EIC detector. These beam tests would most likely be done at either SLAC where one can obtain a high precision beam of electrons with a momentum up to 15 GeV or at Jefferson Lab where the upgraded CEBAF provides electron beams up to 11 GeV.

The prototype setup could be based on that for the JLab NPS, which has an active area of about 6x6 cm<sup>2</sup> including a crystal matrix of PbWO<sub>4</sub> (and PbF<sub>2</sub> to test hybrid configurations of crystals) in a copper frame. A first version of this prototype was recently constructed at JLab using 3D printing technology. The prototype is shown in Figure 16.

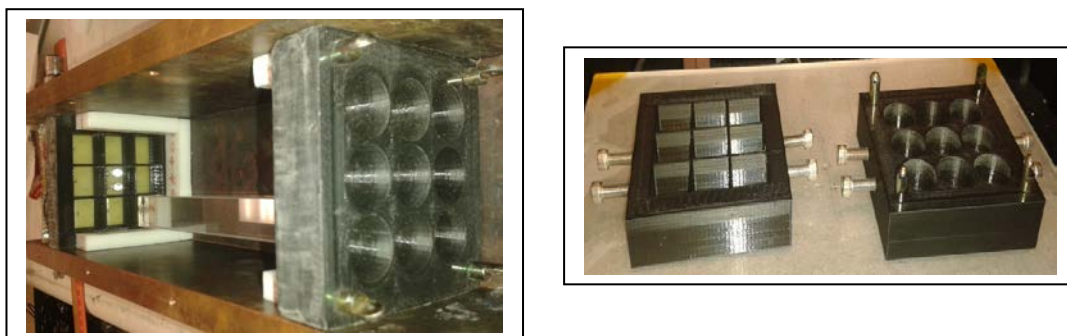


**Figure 16:** Optimized NPS prototype constructed using 3D printing technology.

The readout is done by 19 mm Hamamatsu R4125 PMTs with a JLab developed new active HV base. One could consider using the NPS prototype or a modified version of it, which could provide flexibility in the construction schedule.

As a second stage of testing we will continue to investigate reading out the calorimeter with SiPMs or other sensors with tolerance to radiation and magnetic fields. Our initial results showed that the signal is very small complicating measurements in the lab. We are thus investigating alternatives for SiPM readout with the prototype calorimeter.

### **What are critical issues?**

At this stage, the most critical issues are to have finalized setting up the infrastructure for crystal testing, e.g., at IPN-Orsay, understand systematic effects in our measurements of SIC crystals, and evaluate crystal-to-crystal variation in full-size crystals from Crytur. The construction of a prototype would allow us to study the crystals in test beam and measure the actual energy and position resolution that we could achieve with them. These measurements would provide additional information on crystal specifications and their impact on EIC detector performance.

### **FY2016 Budget Request**

The proposed FY16 budget would allow us to finalize setting up the infrastructure for crystal testing, e.g., at IPN-Orsay and understand systematic effects in the characterization of SIC produced crystals. This activity is synergistic with independent research for the Neutral Particle Spectrometer project at JLab. As part of this project a set of SIC crystals was investigated and the crystal performance seemed to mostly conform to PANDA requirements. A crystal testing setup including optical properties and their homogeneity is being developed at CUA. This is an essential aspect required to quantify the homogeneity of crystals produced at SIC, and thus would provide a measure of the quality that can be achieved by that vendor. The budget would also allow us to procure full-sized crystals from Crytur and evaluate their crystal-to-crystal variation. The company expects to have finalized their setup of four furnaces and cutting and polishing equipment to start the production of full-sized R&D crystals by the beginning of FY16. This timeline fits well with planned crystal R&D activities for FY16. The FY16 budget would also allow us to construct a prototype to study the crystals from either manufacturer in test beam and measure the actual energy and position resolution that we could achieve with them. Further, the prototype would allow us to test a SiPM-based readout system for the crystal inner calorimeter. These measurements would provide additional important information on crystal specifications and their impact on EIC detector performance.

Assuming that our crystal quality tests are completed successfully and one or two vendors capable of producing such crystals have been identified, the crystal calorimeter R&D will focus in subsequent years on the optimization of geometry,

cooling and choices of readout system of the endcap inner crystal calorimeter. Cooling and choice of temperature are important aspects for crystal calorimetry. The choice of temperature balances light output and radiation recovery. Cooling techniques have been explored for PANDA and CMS. The type of cooling and avoiding condensation depend to some extent on environmental factors. Our planned future R&D will explore how cooling could be achieved for the inner endcap calorimeter for EIC. Another reason for cooling is the reduction of noise in the readout system. Our initial studies with a SiPM-based readout have shown significant effects of noise at room temperature emphasizing the need for cooling. Our future R&D activities will also explore if cooling is the optimal choice to reduce readout noise and if it is how to implement such a system.

### R&D Timeline and Deliverables

Deliverable	FY16 by Quarters				FY17 by Quarters			
	Q1	Q2	Q3	Q4	Q1	Q2	Q3	Q4
Procure crystals from Crytur	X	X						
Crystal quality tests	X	X	X					
Radiation Damage studies	X	X	X					
Construct prototype		X	X					
Test prototype				X	X			
Calorimeter configuration				X	X			
Cooling system studies						X	X	X
Readout system				X	X			
Readout noise reduction						X	X	X

### Institution Responsibilities

- CUA - Lead Institution. Coordination of R&D program. Perform crystal quality measurements, construct and test prototype
- JLAB – provides facilities for radiation studies and quality measurements as needed
- BNL - Carry out radiation damage measurements (gamma ray and hadron). Study crystal readout using SiPMs
- Caltech – Perform crystal quality measurements and carry out gamma ray radiation damage studies
- IPN Orsay – procure PWO crystals from Crytur and perform initial crystal quality measurements in collaboration with University of Giessen
- Yerevan Physics Institute – Provides expertise with crystal quality measurements and comparison with other calorimeter crystal types, e.g.,  $\text{PbF}_2$  and existing  $\text{PbWO}_4$

## Funding Request and Budget

**Table 2.** Funding by task

Item	FY16 (\$K)	FY17 (\$)
Procure crystals from Crytur	40	
Gamma ray radiation studies	10	
Hadron radiation studies	5	
Technical Support	5	15
Parts for prototype	10	
Travel	5	15
Parts for cooling system		40
Parts for readout system		30
<b>Total</b>	<b>75</b>	<b>100</b>

**Table 3.** Funding by Institution

Institution	FY16 (\$K)	FY17 (\$k)
CUA	20	30
JLAB		
BNL	10	20
Caltech	10	
IPN Orsay	35	50
Yerevan		
<b>Total</b>	<b>75</b>	<b>100</b>

## Manpower

*Include a list of the existing manpower and what approximate fraction each has spent on the project. If students and/or postdocs were funded through the R&D, please state where they were located and who supervised their work.*

A list of existing manpower is shown below. All of the participants are supported by external funds and not through the EIC R&D program.

### **IPN-Orsay**

G. Charles

G. Hull

C. Munoz-Camacho

### **CUA**

M. Carmignotto

A. Mkrtchyan

T. Horn

### **Yerevan**

H. Mkrtchyan

**BNL**

C. Woody  
S. Stoll

**Caltech**

R-Y Zhu

**External Funding**

*Describe what external funding was obtained, if any. The report must clarify what has been accomplished with the EIC R&D funds and what came as a contribution from potential collaborators.*

Efforts related to crystal studies as described in the proposal were accomplished with EIC R&D funds. Salaries and wages were provided by private external grants from the individual principal investigators, e.g., IPN-Orsay, Yerevan, and the National Science Foundation. Additional funds for logistics related to the Idaho irradiation tests were obtained in collaboration with the Neutral Particle Spectrometer project at JLab.

**Publications**

*Please provide a list of publications coming out of the R&D effort.*

We have presented initial results of our crystal studies at the SCINT15 conference. Journal publications are expected at the conclusion of our studies.

## Subproject Name: BSO Crystal R&D for a Forward Calorimeter at EIC

**Project Leader: Yifei Zhang**

### The planned work and the progress for the report period:

We planned to test the 3x3 BSO prototype with electron beam from 1 to 5 GeV at FNAL. The goal of the beam test is to investigate the performance of the BSO prototype and to study how good the resolution we can achieve with this recently developed BSO crystals provided by SICCAS.

#### 1) Beam test at FNAL.

##### 1.1) Mappings

The followings are determined from cosmic ray test at BNL at the end of last year. One can also find the information from last report (2014 Dec). We used the same mappings for the beam test. In order to be clear, we briefly define the mappings here again.

The crystals classification according to energy deposit and HV connection and channel numbering and are show as Fig.1

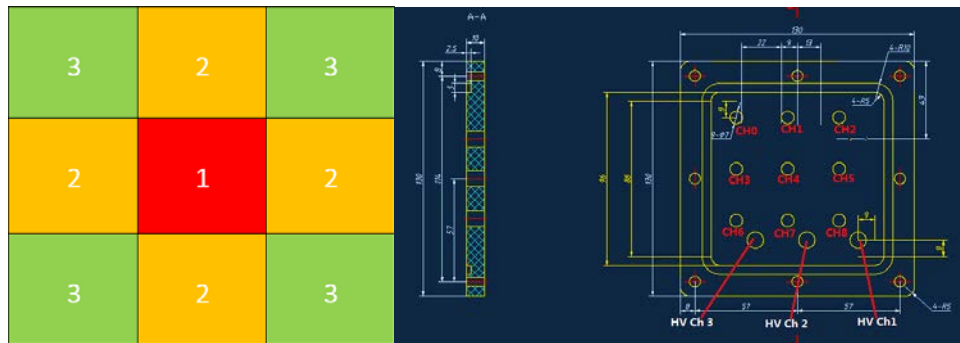


Fig. 1: Crystal classification and Front panel schematic diagram (front view).

Table 1 shows the mapping of crystal number and channel ID. Table 2 listed the crystal LY output and corresponding PMT parameters.

Channel	CH0	CH1	CH2	CH3	CH4	CH5	CH6	CH7	CH8
BSO #	03	11	01	07	08	10	02	06	04

Table 1: Mapping between crystal number and readout channel.

BSO #	01	02	03	04	10	06	07	08	11
LY[pe/MeV]	37.9	43.9	49.8	46.9	53.9	58.4	53.5	86.9	81.2
PMT #	1829	1847	1848	1833	1832	1845	1830	1843	1844
Gain HV=-800V	8.6e5	5.1e5	4.3e5	4.7e5	3.6e5	3.2e5	3.7e5	1.4e5	1.9e5

Table 2: Mapping of crystal number and PMT parameters.

##### 1.2) DAQ system

During the beam test, we used STAR standard QT board for DAQ (provided by HCal group), the mapping of BSO channels to the QT board (#0x13) are shown below. Note the beam direction is out of the paper.

B1/ch0	B2/ch1	A2/ch2
A3/ch3	A4/ch4	A5/ch5
A6/ch6	A7/ch7	A8/ch8

Figure 2 left panel shows the QT board clock and corresponding signals for three channels. The timing information is given by beam counter 1 (BC1) discriminate signal and  $\Delta T = \text{TriggerCrossing\_falling\_edge} - \text{Trigger\_Time}$  as shown in right panel, which shows except the peak around 0, there are large fraction of random shaping time. The peak at 70ns is overflow due to the 70 ns gate width.

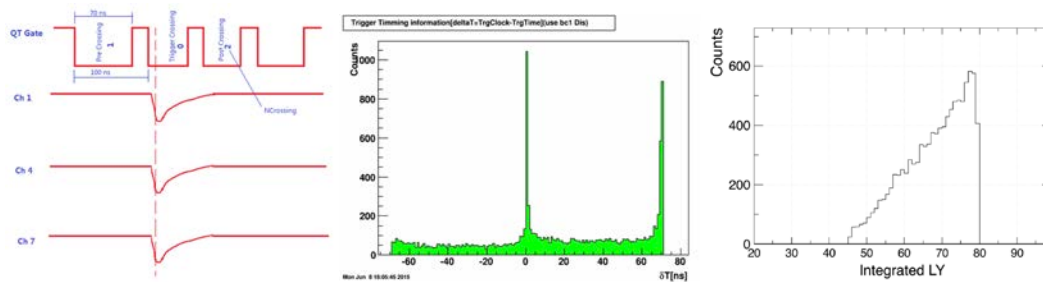


Fig. 2: Left: QT board clock and trigger. Middle:  $\Delta T$  distribution from BC1. Right: Integrated light yield of within 70ns with random trigger.

This 70ns gate width with random trigger results in a reduction of integrated light yield, see right panel of Fig.2. This is one of the reasons that make the energy resolution worse.

### 1.3) Setup the detector

Each channel of the prototype was tested and confirmed working well before the beam test when arrived at FNAL. Figure 3 shows a picture of the pre-testing.



Fig. 3: The prototype during the pre-testing.

The frame box of the prototype was asked to open for safety check. Figure 4 shows the inside details during the safety check. Unfortunately, one of the channels (CH6) was found dead probably due to connection lost or damaged after the safety check and there was no signal observed afterwards. We do not have sufficient time to fix it, thus CH6 was dead all through the beam test.



Fig. 4: The inside view of the prototype opened for safety check.  
 Left: The base board and the PMTs. Right: The 3x3 BSO crystal array.

The prototype is located on the top of the HCal during the beam test. Both of them are fixed on the platform, which can move horizontally and vertically, see Fig. 5 left. The test system layout is shown as Fig. 5 right panel.

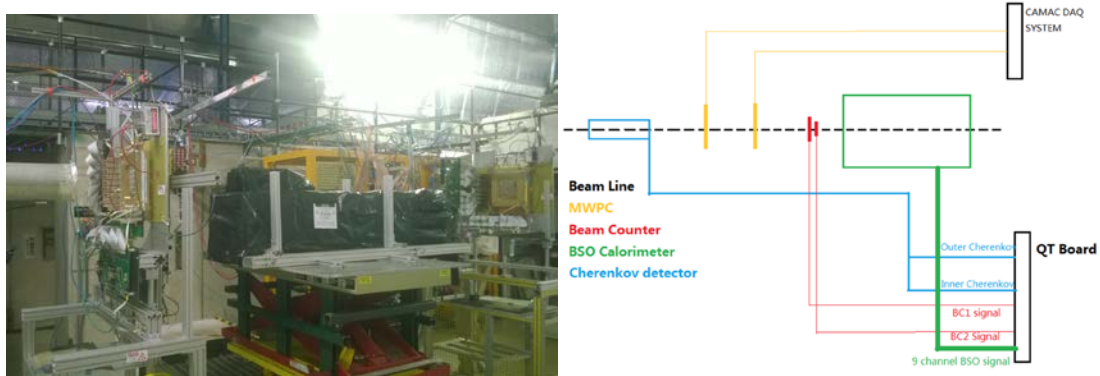


Fig. 5: The test system and its layout.

#### 1.4) Beam profile

The beam profile is poor at low energy. Figure 6 shows the online plot for the beam position for 5 (left) and 3 (right) GeV at MT6WC2 where our prototype located. The mean and width of the beam along horizontal and vertical directions were obtained from the online monitor, which is summarized in Table 3.

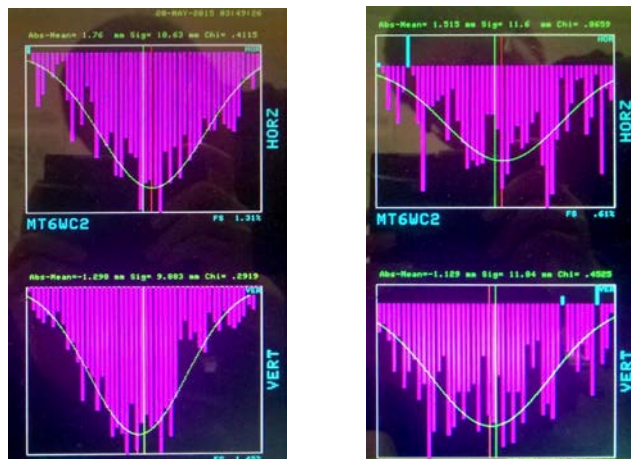


Fig. 6: The beam profile for beam energy = 5 (left) and 3 (right) GeV.

Energy	5 GeV	3 GeV
VERT Mean	1.29 mm	1.129 mm
VERT Sigma	9.003 mm	11.84 mm

HORZ Mean	1.76 mm	1.515 mm
HORZ Sigma	10.63 mm	11.6 mm

Table 3: Mean and sigma for the beam profile at 5 and 3 GeV.

The beam momentum resolution below 15 GeV is very poor. According to the information from the accelerator, the  $\sigma_p = (2.7 \pm 2.7)\%$  below 5 GeV. However, from the PBGlass check, the beam momentum resolution at low energy is about 5.7% with large uncertainty.

### 1.5) Results from the beam test

The ADC from BC1 and BC2 are required to be larger than 100 and 50, respectively. The ADC in each crossing is required to be less than 4000. The raw ADC and timing distributions for 9 channels (CH0 – CH8) from Run15140012 at 5 GeV are shown in Fig. 7. There is no signal (some fake entries) from CH6 as we mentioned previously. The small signal in CH4 (the center of the prototype) is due to that we used a filter paper for protection since most of the beam time is with high energy and the PMT will be saturate out of the dynamic range. Except CH6, the timing distributions of the other 8 channels are reasonable.

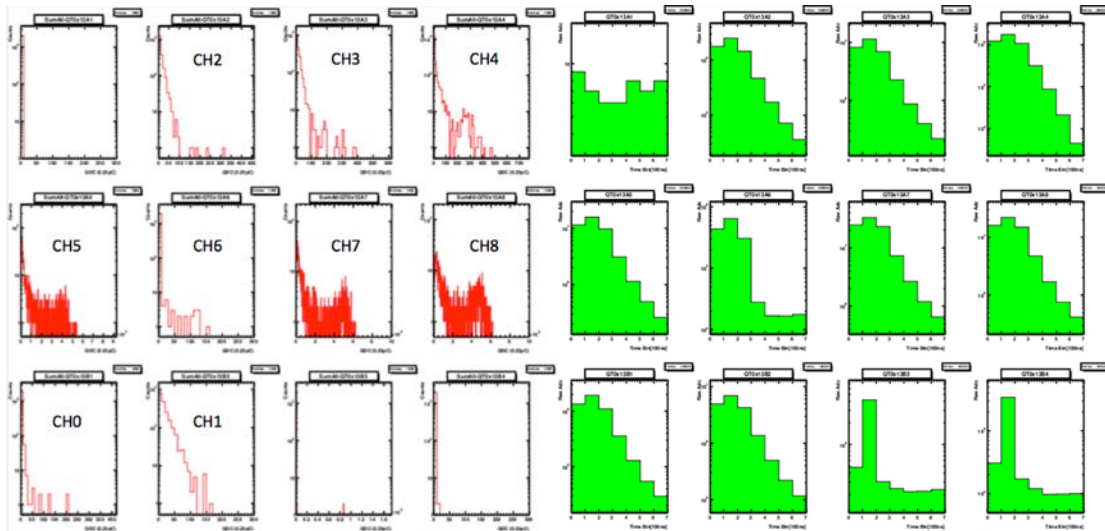


Fig. 7: The raw ADC (left) and timing (right) distributions for 9 channels.

The total raw QDC spectra from sum of the 8 channels for 5, 3 and 2 GeV are shown from left to right in Fig. 8.

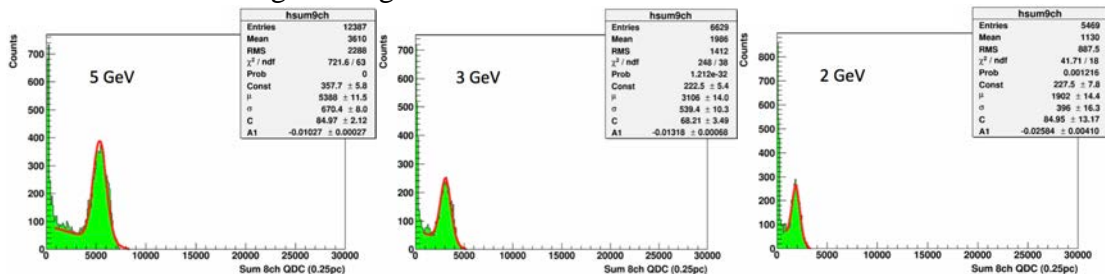


Fig. 8: The raw QDC spectra from sum of the 8 channels.

The raw energy resolution is obtained for three incident energies without calibration. The calibration is still on going. Figure 9 shows the very preliminary result of the raw energy resolution versus incident beam energy.

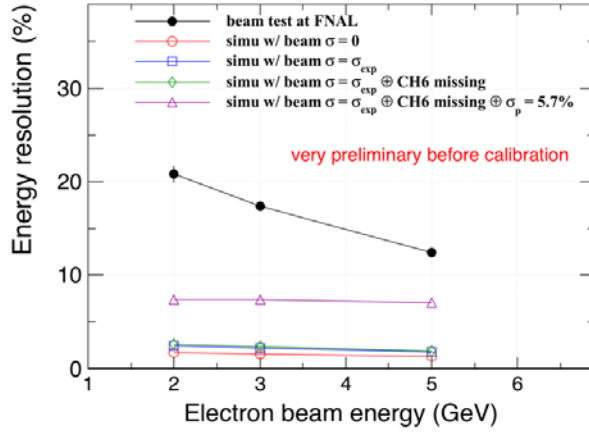


Fig. 9: Very preliminary energy resolution as a function of incident electron beam energy.

## 2) Simulation

The dead channel, beam spread and momentum smearing will lead different amount of missing energy during the beam test. To understand this, we did the Geant4 simulation for the 3x3 module with the same incident electron beam energy as the experiment. The fraction of missing energy versus the incident beam energy is shown in Fig. 10 (a). Red open circles are the result with beam without any spread, which means the ideal case that the 3x3 module will have ~10% energy missing. Blue squares represent the result with beam width according to measured values as listed in Table 3. The result with dead CH6 marked out is shown as green diamonds. Magenta triangles are with additional momentum smearing with  $\sigma_p = 5.7\%$ .

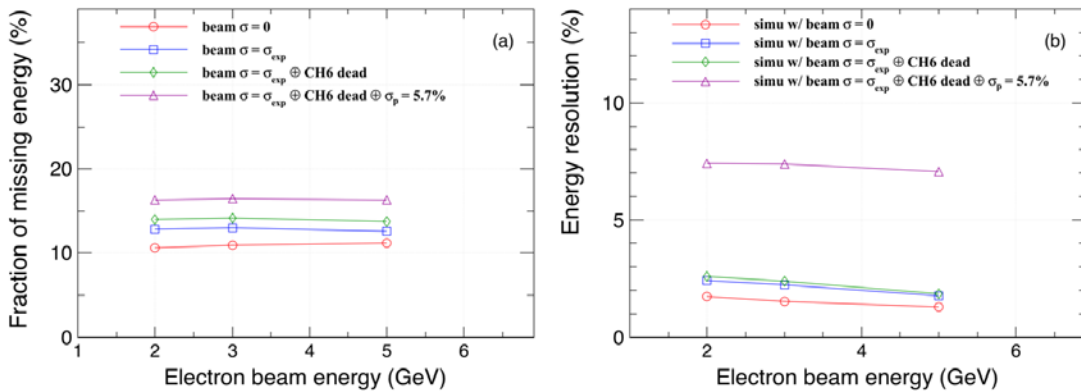


Fig. 10: Fraction of missing energy (a) and intrinsic energy resolution (b) as a function of incident electron beam energy.

In the Geant4 simulation, the beam is fixed to incident along center of the module. However, the beam position is not exact at center during the beam test. The positioning calibration with MDC is still on going. In addition, there is a filter used in the center channel (CH4), the reduction on the photon signal also need to study with muon events. The intrinsic energy resolution from simulation is shown in Fig. 10 (b). It is hard to compare with data without correction on beam position, different gain for each channel and photon reduction of the filter.

## **What was not achieved, why not, and what will be done to correct?**

The original plan is to have final beam test result compared with simulation. However, the beam test schedule was delayed and beam test was just finished. The beam profile is poor and calibration work is still on going.

What do we learn from the beam test?

The beam test at FNAL is an effort to characterize the detector performance despite the poor beam condition. The data is still under calibration and simulations for understanding the large deviation of the raw data and simulation. From this beam test, we learned a few reasons that caused the worse energy resolution:

a) The beam spread is on the order of  $\sigma \sim 10$  mm. The beam momentum resolution is around 5.7%. The beam rate is not stable at low energy and we are not able to have sufficient data, especially for 1 GeV. It is hard to characterise the crystal intrinsic performance with such beam condition this time. Another beam testing possibly at SLAC is needed to determine the characteristic performance of the crystals.

b) The filter paper should not be used in the central channel, since most of the energy deposited in that crystal. It was used for protection under high beam energy, since most of time is with high energy for STAR HCal testing. But later on we do not have sufficient time to take the filter out. This leads to a large fraction of energy missing and is hard to be calibrated.

c) 70ns gate width using the QT board with random trigger results in some fraction of light yield loss. We may need our own DAQ system next time.

In addition, we expected to have some more new crystals from SICCAS, however the production plan was delayed.

### **Future**

- 1) Finish the calibration of the beam test data and try to understand the big difference between data and simulation. Probably need further beam test with better electron beam quality (e.g. SLAC) for characterizing the performance of the crystals.
- 2) Possible study on the BSO performance with SiPM readout.
- 3) Test new crystals when produced by SICCAS.

**Project ID:** eRD1  
**Project Name:** EIC Calorimeter Consortium  
**Sub Project:** Shashlyk Calorimeter R&D at UVa  
**Project Leader:** Xiaochao Zheng  
**Contact Person:** Xiaochao Zheng (xiaochao@jlab.org)  
**Date of Submission:** June 15, 2015

# Simulation and Construction of Shashlyk-Type Electromagnetic Calorimeters for the Electron-Ion Collider

June 14, 2015

Kai Jin, Nilanga Liyanage, Vincent Sulkosky, Nguyen Ton, Xiaochao Zheng<sup>1</sup>  
*Department of Physics, University of Virginia, Charlottesville, Virginia 22904, USA*

Guy Ron  
*Racah Institute of Physics, Hebrew University of Jerusalem, Jerusalem, Israel 91904*

Alexandre Camsonne  
*Thomas Jefferson National Accelerator Facility, Newport News, Virginia 23606, USA*

Wouter Deconinck  
*College of William & Mary, Williamsburg, Virginia 23187, USA*

Tim Holmstrom  
*Longwood University, Farmville, Virginia 23909, USA*

Jin Huang  
*Brookhaven National Laboratory, Upton, NY 11973-5000, USA*

Zhiwen Zhao  
*Duke University, Durham, North Carolina 27708, USA*

## Abstract

Electromagnetic calorimeters (Ecal) constitute an important part of the detector package for the Electron-Ion Collider (EIC). The shashlyk-design is a type of sampling calorimeter that provides a reasonable energy resolution and a high radiation resistance, and at a lower cost than crystal calorimeters. We propose here a first step towards the R&D study for building shashlyk calorimeters for the EIC. For the first year, we will carry out preliminary simulations to determine a basic design of shashlyk calorimeters for the EIC's outer electron and hadron endcap calorimeters, and to study the feasibility of using shashlyk for the barrel calorimeter. We will also conduct preparation work towards shashlyk module construction, focusing on testing the optical and mechanical properties and the radiation hardness of the scintillator and absorber components of the module. In addition to using scintillators produced with traditional methods, we will incorporate a possibly innovative method which is 3D-printed scintillators. 3D-printed scintillator parts will allow us to efficiently carry out the prototyping process and to directly produce projective-shape modules, the latter may be important for the EIC. The proposed project will work for both eRHIC and MEIC.

The requested funding period is for one year and the funds will be used to cover the necessary test setup, material and supplies, and the manpower needed to conduct this R&D research. Once we have determined the design and have obtained the basic data on properties of the scintillator and the absorber components, we will proceed to prototype construction at the next funding cycle, focusing on the two endcap calorimeters and the possibility of producing projective-shape modules.

---

<sup>1</sup>email: xiaochao@jlab.org

# 1 Calorimeter Needs for the EIC and the Proposed Study

Calorimeters provide measurements of particles' energy in medium- and high-energy experiments. They often also provide particle identification, triggering, and moderate tracking information. For collider experiments such as those being carried out at the large hadron collider (LHC) and being planned for the electron-ion collider (EIC) [1], both hadron and electromagnetic calorimeters are needed. Typical energy resolutions required for Ecal varies between  $(1 - 2)\%/\sqrt{E}$  to  $12\%/\sqrt{E}$  with  $E$  in unit GeV/c, while the resolution that can be achieved for Hcal is much larger, in the order of  $100\%/\sqrt{E}$ . Other constraints on collider calorimetry include compactness, radiation hardness, and sometimes a projective shape may be desired.

## 1.1 Shashlyk-Type Calorimetry

Many different technologies have been developed for calorimetry in the past century. The commonly used options include lead-glass, NaI and CsI. The energy resolution is moderate, varying from  $5\%/\sqrt{E}$  to  $(1.5 - 2.0)\%/\sqrt{E}$  for NaI and CsI. However these are not radiation hard and cannot be used under the harsh environment at colliders. Crystal calorimeters such as LSO,  $\text{PbWO}_4$  or  $\text{PbF}_2$  are radiation hard and with excellent energy resolution, however their cost is often too high for collider experiments where large volumes of calorimeter are needed. A relatively new technology is based on samplings of electromagnetic showers developed by the particle, such as SPACAL or Shashlyk-type calorimeters. They provide a reasonable energy resolution ( $5\%/\sqrt{E}$  is achievable) with a moderate cost. In the following we will focus on the shashlyk sampling technology.

Shashlyk-type calorimeter modules [2, 3, 4] are made of alternating layers of an absorber and scintillator. Scintillating light is guided out from the module by wavelength-shifting (WLS) fibers that penetrate through all layers and is detected in PMTs or SiPMs. The WLS fiber ends that are opposite to the readout are typically coated with a reflective layer using aluminum sputtering to improve the light yield and the longitudinal uniformity. The shashlyk technique has been used successfully in recent LHC experiments. It is a cost-efficient alternative to crystal calorimeters while providing a comparable radiation resistance in the order of  $10^6$  rad. On the other hand, the drawbacks of the shashlyk method include high costs of prototyping due to the traditional methods used for producing the module parts (injection-molding for the scintillator layers and stamping for the absorber layers); the complexity of the module assembly process; the difficulty to make the modules in projective shapes due to the fixed size and shape of module parts; and the limitation on the energy resolution due to non-uniformity of both absorber and scintillator sheets.

## 1.2 Shashlyk EM Calorimeters for EIC

Figures 1 and 2 show respectively the conceptual design for the interaction region of both ePHENIX at RHIC [6] and MEIC at JLab [7, 8]. In the following we will describe the general requirement of Ecal for both cases.

For ePHENIX, we will need:

- A central/barrel Ecal, needs to be compact radially with a moderate  $12\%/\sqrt{E}$  resolution. Because ePHENIX will be built upon the upgrade sPHENIX, the central Ecal needs to be projective with fine lateral segmentation [6]. Currently the top choice is the tungsten sci-fi design with  $2.5\text{cm} \times 2.5\text{cm}$  segmentation and occupies about 25 cm of radial space including 13 cm of the detector itself and 12 cm of readouts [9]. However, the radial space constraint is ultimately determined by the coil size, which extends beyond 25 cm. A shashlyk design is therefore possible from the space point of view, provided it can be projective. A careful study is needed to develop the shashlyk design and compare to the existing tungsten sci-fi design in both cost and performance.
- A forward (electron direction) Ecal that requires a  $(1 - 2)\%/\sqrt{E}$  resolution for the small angle region and a  $(5 - 6)\%/\sqrt{E}$  for the large angle region. The different requirement is due to the angle dependence of tracking. For small angles, the precision in tracking will be poor and one

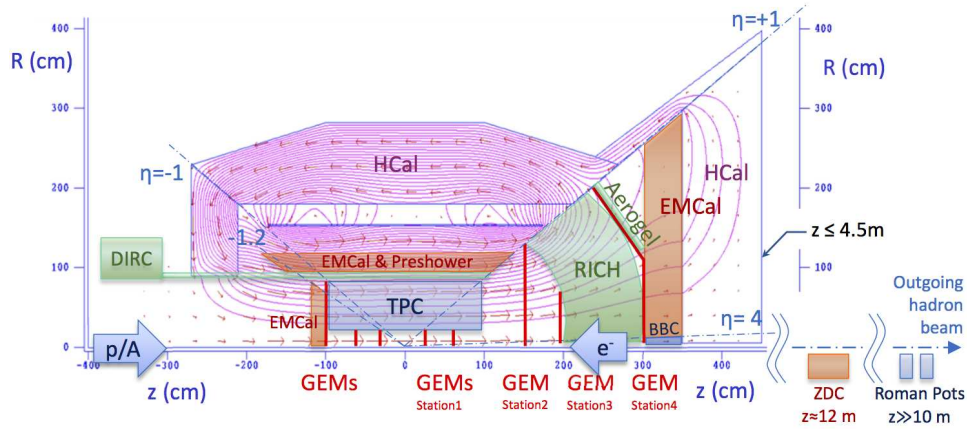


Figure 1: Detector package for ePHENIX [6]. The three EM calorimeters are shown in red.

needs Ecal to provide both PID and the absolute energy information of the particle. For large angles, the precision in tracking is significantly better and the Ecal is needed only for PID, for which a moderate energy resolution will be sufficient. For the inner Ecal the choice would be crystal (lead-tungstate) [10]. But for the outer Ecal a shashlyk design may be the best choice.

- A backward (hadron direction) Ecal that requires a moderate  $(12 - 15)\%/\sqrt{E}$  resolution. A shashlyk design may be the best choice.

The electron and the hadron Ecals do not need to have projective-shape modules but a projective design will help with PID and energy resolution compare to a non-projective one.

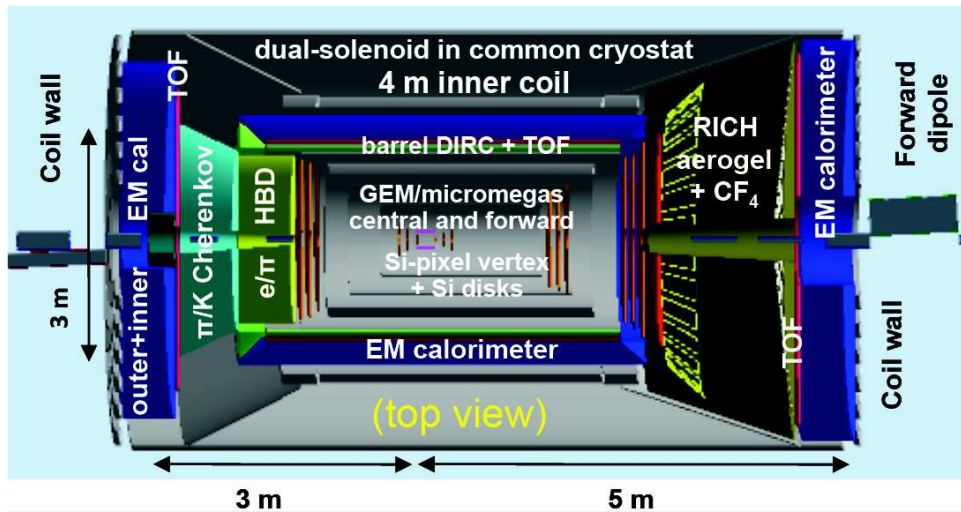


Figure 2: Detector package for MEIC's interaction point [7, 8]. The three EM calorimeters are shown in blue.

For MEIC, we will need:

- A central (barrel) Ecal, needs to be compact radially with a moderate  $12\%/\sqrt{E}$  resolution. Currently a 25-cm radial space is reserved for the Ecal including readout. This constraint is directly from the location of the magnet coil and is therefore more stringent than for ePHENIX.

The tungsten sci-fi design for ePHENIX will work here, although one does not need the fine lateral segmentation. Another possible choice is to use a lead sci-fi design which is identical to the JLab Hall D/GlueX Ecal. However, a shashlyk design is not yet out of the question. A careful study is needed for the feasibility of a shashlyk design that fits into the tight radial space, and to compare cost with the other two choices.

- An electron-direction endcap Ecal. Similar to the ePHENIX case, it will consist of an inner(-radius) crystal (lead-tungstate) Ecal plus an outer(-radius) Ecal. Again the requirement on the energy resolution of the outer layer is moderate and a shashlyk design is possible.
- A hadron-direction endcap Ecal. The energy resolution required is  $(5 - 6)\%$  and a shashlyk design is possible.

Unlike sPHENIX's barrel Ecal, the MEIC barrel Ecal does not need to be projective. Overall none of the Ecal's for MEIC needs to be projective. However, a projective design will certainly improve the energy resolution compared to a non-projective design.

As one can see from above, Shashlyk calorimeter can be used for both the hadron Ecal and the outer-radius electron Ecal for the EIC. It can also possibly be used for the barrel Ecal although a more careful study is needed to study its feasibility. On the other hand, no simulation has been done to establish the basic design parameters for EIC's shashlyk Ecal's and to estimate their costs, and to investigate if shashlyk modules from other projects (either existing or planned) can be used. In addition, the expertise in shashlyk calorimeter construction lies mostly in Russia (IHEP and ITEP). Only a couple of university groups in the US currently have experience constructing shashlyk modules, but they are all outside the nuclear physics community. It is urgent to gain experience and obtain expertise in shashlyk module construction within the EIC community.

### 1.3 The Proposed Study

We propose here a first step in the R&D of shashlyk calorimeter design and construction for the EIC. On the design R&D, we will carry out preliminary simulations to determine the basic parameters of EIC's hadron and outer-electron endcap Ecal's, and will study the feasibility of using shashlyk for the barrel Ecal. On the construction R&D, we will start from testing the optical and mechanical properties and radiation hardness of the scintillator parts for shashlyk modules. In addition to using scintillator parts produced from traditional methods, we would like to incorporate studies of 3D-printed scintillators which is now available from some industrial R&D programs as well as from universities.

Although 3D-printed scintillators are only a component of the proposed study, it is a relatively new technique and is not well known. Therefore we will describe it here briefly and its status and potential in detail in Appendix A. The most appealing advantages of 3D-printing are the fast turn-around time, the possibility of in-house prototyping and production, and the ease of changing the product shape and size during production which is needed for producing projective-shape shashlyk modules. In the longer term, 3D-printing could provide better control over layer uniformity (layer thickness of 3D printing can be at the micron level) which is crucial for reducing the energy resolution of the shashlyk calorimeter. Depending on the printer used and possible modifications that can be made to the commercially-available printer, one could also simplify the module assembly process.

The scintillators produced with traditional methods will be provided by the Chinese Beijing High-Energy Kedi company<sup>2</sup> and Eljen Technology<sup>3</sup>. The 3D-printed scintillators will be provided also by two parties: 1) made in-house at the College of William and Mary; and 2) the R&D department of Stratasys, a leading 3D-printing company<sup>4</sup>. We will start from the general transparency, light yield, and mechanical strength and properties of simple-shape samples. Then we will proceed to testing preshower modules which are made of a single piece of 20mm-thick scintillator with WLS-fiber

---

<sup>2</sup><http://www.gaonengkedi.com/>

<sup>3</sup><http://www.eljentechnology.com/>

<sup>4</sup>[www.stratasys.com](http://www.stratasys.com)

embedding, for which we already have data on three different prototypes produced with traditional methods, including prototypes from Beijing HE-Kedi and Russian IHEP. As a third step towards shashlyk module construction, we will test the light yield, transparency, and the mechanical strength of thin scintillator sheets needed for constructing shashlyk modules. If all goes well, we will place the samples in a high radiation area and then repeat the light yield test to obtain data on their radiation hardness. Related to 3D-printed scintillators, we will explore the optical clarity and light transmission of 3D-printed light guides made from commercially available optical-quality materials (“veroclear” and “t-glase”). We will also experiment with aluminum-sputtering which has been used to attach reflective mirrors to WLS fiber ends.

Within the proposed one-year funding period, we hope to achieve a conceptual design of shashlyk calorimeters for the EIC. In terms of hardware work, we hope to show that the scintillator parts from both traditional methods and from 3D-printing have the mechanical strength and the light yield required for shashlyk module construction. These initial tests will also provide hands-on experience on working with thin scintillators and absorber (lead) parts, which are valuable by themselves and will allow us to design the shashlyk modules and the assembling process more realistically. If 3D-printed scintillators work, it may open up the possibility of fast and in-house prototyping, and producing projective-shape shashlyk modules with ease.

## 2 Shashlyk-Type Calorimetry – Current Status and Limitations

As mentioned earlier, shashlyk calorimetry [2] is a type of sampling detectors that provide a cost-effective alternative to radiation-hard crystal calorimeters. Shashlyk-type calorimeter modules are made of alternating layers of an absorber (such as lead or tungsten) and a scintillator. Particles are efficiently slowed down and stopped by the absorber layers, and the scintillator layers sample the amount of showers produced. Scintillating light is guided out by wavelength-shifting (WLS) fibers penetrating through all layers of the module. In a simple model where we assume the shower particles share the energy evenly, the energy resolution is determined to the first order by [11, 12]

$$\left(\frac{dE}{E}\right)_{shashlyk} = \frac{1}{\sqrt{N_s}} \quad (1)$$

where

$$N_s = F(\xi) \cos \theta_{MS} \frac{E}{E_c} \frac{X_0}{\Delta t} \quad (2)$$

with  $E$  the particle energy,  $E_c$  the critical energy ( $E_c \approx 550 \text{ MeV}/Z$  for electrons),  $X_0$  and  $\Delta t$  the radiation length and the layer thickness of the absorber. In Eq. (2),  $E/E_c$  is the total number of shower produced by the particle and  $X_0/\Delta t$  represents how often the shower maximum (within one radiation length) is being sampled by the absorber/active layers,  $\theta_{MS}$  is the multiple-scattering angle, and  $F(\xi)$  is a function depending on the detection threshold. If the threshold energy is small and at the MeV level or below,  $F(\xi) \approx (0.7 - 1.0)$ . For electrons of  $(1 - 10) \text{ GeV}$  initial energy, the shower maximum develops at  $(7 - 10)X_0$ , and an additional  $(7 - 9)X_0$  is needed to absorb  $> 95\%$  of energy carried by all photons that are originated at the shower maximum. This means a total absorption Ecal need to be at least  $(14 - 16)X_0$  thick. For shashlyk modules constructed from 0.5-mm thick lead sheets, using  $E_c \approx 8 \text{ MeV}$  and  $X_0 \approx 0.54 \text{ cm}$  for lead, the simple calculation of Eqs.(1-2), ignoring terms  $F(\xi)$  and  $\cos \theta_{MS}$ , gives an energy resolution of  $\approx 3.3\%/\sqrt{E}$ . The thickness of the scintillator would affect energy resolution to the second order. In reality, the actual energy sharing between shower particles is not even and the number of showers is smaller than Eqs.(1-2). Detailed simulation for modules made of 0.5-mm lead and 1.5-mm scintillator sheets gives  $\approx 5\%/\sqrt{E}$ .

Shashlyk-type calorimeter has been widely used in experiments at the LHC, including ATLAS, ALICE and LHCb. On the other hand, the construction of Ecal modules is labor-intensive and prototyping is expensive due to the complexity of parts. Figure 3 shows a possible design of the absorber and the scintillator sheets for a hexagon-shape shashlyk module. The lateral size is  $100 \text{ cm}^2$  with

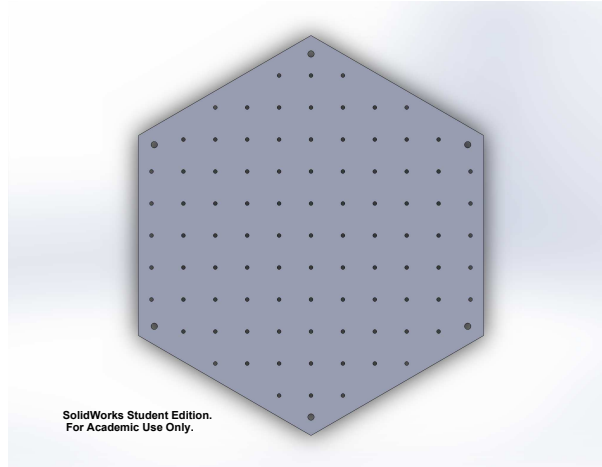


Figure 3: A typical shashlyk module layer design.

93 holes spaced uniformly across the surface to accommodate the WLS fibers. Because of the large amount of holes, scintillator sheets are usually produced by injection-molding, for which the expertise resides almost solely in Russia (Beijing HE-Kedi does do injection molding but we do not know of any shashlyk calorimeter constructed using scintillators from this company, and the following discussions apply to all injection-molding-based productions). Each mold typically cost \$30k which makes up the bulk part of the prototyping cost. Although for mass production the mold cost is not as significant, the high cost of prototyping makes fine adjustments to the design difficult. A second difficulty common to shashlyk module design and construction is that the size of the scintillator sheet is determined by the mold. The fixed size of the mold makes it nearly impossible to construct shashlyk modules of projective shape. (For example to construct the LHC/ALICE modules [5] which are semi-projective, scintillator sheets of a fixed size were produced using injection molding and then cut down to 76 different sizes individually.) Both difficulties also apply to the lead (absorber) sheets which are produced by stamping for large quantities. Although the stamping technique is available in the US and the stamping tool can be made of fixed hole positions with variable outer shape and size, the position and the size of the holes cannot be changed and each stamping tool can cost as much as \$15k, again making prototyping cost very high.

Once all sheets are manufactured, they are assembled on a specially-designed assembly stand. Intensive care is spent on designing the assembling stand such that all holes are aligned. The assembling process itself is highly-technical, tedious, and labor-consuming. For example the LHC/ALICE Ecal construction of 16,000 modules (4,000 “assemblies”) took about 3 years by ten full-time technicians and students.

Performance-wise, because of the production technique of the sheets, there is a limit on how thin the sheets can be manufactured and how uniform the thickness is. Typically, lead sheets as thin as 0.3 mm can be manufactured with a tolerance of  $\pm 0.025$ mm. The tolerance of scintillating sheets can only reach a fraction of mm. For thinner sheets, non-uniformity in the thickness gives rise to a constant term in  $dE/E$  that limits the overall resolution to  $(3 - 5)\%/\sqrt{E}$  regardless of the design layer thickness. If the physics program requires better energy resolution, crystal Ecal must be used which costs one order of magnitude higher than the Shashlyk design.

While the focus of this R&D proposal is to establish the shashlyk Ecal design for the EIC and to gain experience towards shashlyk module construction, the 3D-printed scintillator study will potentially help to address the limitations of existing construction method described above. For details please see Appendix A.

## 3 Proposed Simulation and Test Plan

### 3.1 Simulation for the EIC Shashlyk ECal

We would like to conduct preliminary simulation for the EIC shashlyk Ecal(s). We will start from the hadron and the outer-electron endcap Ecal. We will determine the basic longitudinal design to reach respectively a  $(10 - 12)\%/\sqrt{E}$  resolution for the ePHENIX hadron Ecal and a  $5\%/\sqrt{E}$  resolution for the MEIC hadron Ecal and the outer-electron Ecal for both ePHENIX and MEIC. For MEIC both endcap Ecal also have a thickness constraint. Meanwhile we will study the feasibility of using shashlyk design for the barrel Ecal. As one can see from the previous section, if a 0.5-mm Pb/1.5-mm scintillator layer design can provide a  $(5 - 6)\%/\sqrt{E}$  resolution, simple scaling of the lead layers tells us that  $(10 - 12)\%/\sqrt{E}$  resolution may be achieved using a 2.0-mm Pb/1.5-mm scintillator design and a  $18X_0$  Ecal will be 17.5 cm in thickness (50 layers each). This is smaller than the 25-cm radial spatial constraint and leaves room for readouts. Of course, a thorough study is needed to fully understand the energy resolution and to estimate the cost. And for ePHENIX case, ultimately whether we can use a shashlyk design for the barrel Ecal will depend on if we can produce projective-shape modules, which in turn may depend on whether 3D-printed scintillators can be used. In addition to the longitudinal design, we need to also determine the transverse segmentation (module lateral size) which will be a determining factor in the cost estimate. However, the module lateral size can simply be about one Moliere radius since for the luminosity of EIC there is no strong constraint on the module size for suppressing the background.

### 3.2 Mechanical Properties of Scintillator Parts

We propose to measure the following mechanical properties of the scintillators: compressive strength, shear strength, and possibly also tensile strength, Young's modulus and shear modulus. The focus will be on the compressive strength because shashlyk modules from LHC ALICE and LHCb experiments were all made by compressing the scintillator and the lead sheets with a 500 kg force. This requires a  $5 \times 10^5$  N/m<sup>2</sup> compressive strength on the scintillator (no safety factor included). Shear strength will be important if modules are stacked together. Scintillator samples of different shapes and sizes will be used depending on the quantity measured and the test setup. For scintillators made from traditional methods, we will carry out this measurement only for samples without public data (that is, we will focus on scintillators from Beijing HE-Kedi). For 3D-printed scintillators, we may need to iterate multiple times with StratasyS to improve the mechanical properties.

After the initial tests using simple-shaped samples, we will test the compressive strength of shashlyk scintillator sheets as shown in Fig. 3 using samples produced from both traditional methods and 3D-printing. Then we will sandwich the scintillator sheets with lead or tungsten sheets to test the combined strength. Note that the requirement on the scintillator strength may defer between different absorbers, as lead is significantly softer than tungsten.

We hope to find all necessary equipment in the physics and the engineering departments at the University of Virginia. But we will include a \$2k in the budget to cover material and supply.

### 3.3 Transparency and Light Yield Test Using Rectangular Blocks

We will test the transparency of both the light guide and the scintillator using samples of simple rectangular shape, blue LEDs, and a spectrophotometer from the UVa/physics demo lab. For the light yield test, we will optically couple the sample directly to a PMT and measure the MIP response using cosmic rays. 3D-printed samples of the scintillator will be provided by StratasyS or made in-house at William and Mary, while we will 3D-print our own light guide samples for the light guide study. The light guide material and a FDM 3D-printer will be procured using Prof. Zheng's other funds. Samples of scintillators and light guides produced from traditional methods will be measured as well to provide the baseline.

### 3.4 Preshower Transparency and Light Yield Test

A longitudinal segmentation of Ecal into a preshower and a shower portion will significantly help with particle identification. Although it is not clear if we will need preshowers for the EIC (this will be one of the simulation goals), we include tests of preshower samples here because the UVa group has already had extensive experience testing its light yield using prototypes from different vendors, and thus it is straightforward to test new samples and compare with existing data. The preshower design to be used is shown in Fig. 4, which is a 20-mm thick scintillator tile with WLS fiber embedded on the surface to guide out the light. We have already tested preshower prototypes of this design made of different scintillating base materials including polyvinyltoluene(PVT) (Eljen), polysterene (IHEP), and phenylethene (Beijing HE-Kedi). All three prototypes gave  $\approx 80$  photoelectrons when two 1-mm diameter Kuraray Y11 fibers are used (each embedded in the groove 2.5 turns) and read out using typical PMTs. We will carry out the light yield test by both coupling a PMT directly to the side of the prototype, and by WLS-fiber embedding. We will compare results from the 3D-printed sample with all other three existing prototypes. This cosmic test of the 3D-printed Preshower module will provide the first characterization of detector performance using 3D-printed scintillating material.

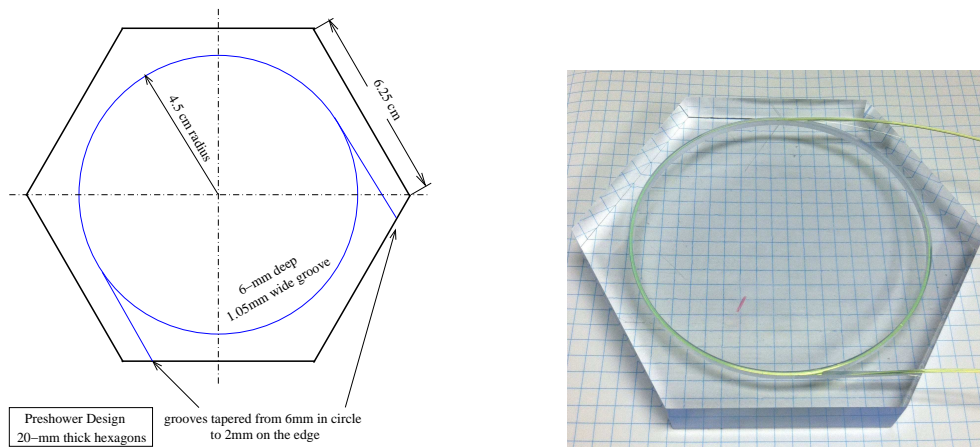


Figure 4: Proposed preshower module for testing. Left: schematic design for the preshower tile. The grooves are for embedding the WLS fibers; Right: a preshower tile produced by Beijing HE-Kedi company that we already tested.

### 3.5 Shashlyk Sheet Light Yield Test (“Hedgehog” Test)

To examine the light-yield quality of the 1.5-mm thick scintillator sheets for shashlyk module construction, we plan to set up a “hedgehog” test where 93 WLS fibers are inserted into the holes of the scintillator sheet, see Fig. 5. The inserted fiber ends should be just above the holes. To increase light yield, a single mirror may be attached to the scintillator’s top surface. The other fiber ends are grouped and coupled to a 2-in dia PMT. Response to cosmic rays will be measured. For scintillators produced with traditional methods, we plan to procure 5 each from Beijing HE-Kedi and Eljen. 3D-printed samples of the scintillator will be provided by StratasyS or made in-house at William and Mary. If the new samples has a comparable light yield as the polysterene-based ones (which we will know from the preshower test), we expect the MIP response to be about 12 photoelectrons which should be straightforward to measure. Measurement of light yield below 2 photoelectrons will be difficult, but in that case the light yield of the new sample will be too low to be useful for detector construction. Similar tests have been used by LHC collaborations to screen the scintillator parts in their shashlyk Ecal construction, and we expect this test to be part of the construction for EIC’s shashlyk Ecal as well.

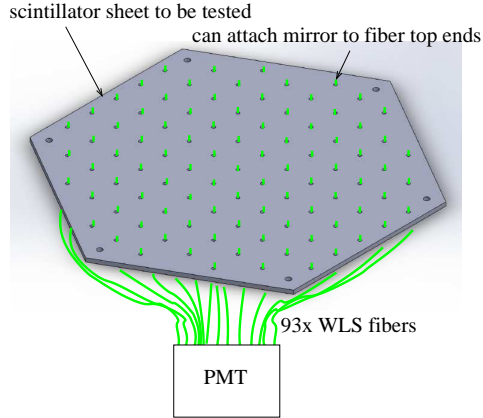


Figure 5: Hedgehog test to determine the cosmic light yield of individual shashlyk scintillator sheets.

### 3.6 Radiation Hardness Test

Once we have established the initial data on the mechanical properties and the light yield of the scintillator samples, we will place the samples in a high radiation area at Jefferson Lab. Then we will conduct the tests again to study the radiation hardness of the samples.

## 4 Budget Request

We request here funds for one quarter of a postdoc, one-half academic year graduate student stipend, material and supply necessary for the proposed tests, and for possible travel to BNL.

Item	cost
5 Eljen EJ-205 shashlyk sheets	\$1,570
5 Beijing HE-Kedi shashlyk sheets	\$1,000*
10 lead layers (Kolgashield) for the combined mechanical test	\$800
Simple-shape scintillators as references (Eljen)	\$1,000*
Light guides as references (Eljen)	\$1,000*
Two scintillator bars (Eljen) for triggering the cosmic test	\$1,400
Readout PMTs for the cosmic test (2 R11102)	\$800
Other material and supply	\$2,000
Travel	\$1,000
One quarter postdoc support (incl. 28% F.B.)	\$17,910
Graduate student, one-half A.Y. stipend	\$19,158/2=\$9,579
Total Request (direct only)	\$38,059
Total Request (including 58% UVa F&A cost)	\$60,133

Table 1: Funding request for the proposed research. Numbers with the \* sign are rough estimates (without quotes). Note the graduate student's health insurance and tuition will come from Prof. Zheng's research funds. Some of the hardware and parts needed for the test, such as a FDM 3D-printer and t-glase for printing the light guide, will come from Prof. Zheng's other resources. For the absorber sheets needed for the combined mechanical tests, we only included costs for the lead sheets because we have not found a vendor to produce the needed tungsten sheets.

While most of the tests can be conducted by graduate students, the GEANT-4 simulation and the radiation hardness test will require the expertise at a postdoctoral level. The postdoc to be supported partially by the requested funding here is Dr. Vincent Sulkosky. Dr. Sulkosky is currently supported half-time by Prof. Zheng's DoE grant and he has extensive experience working with scintillators and detectors in general, including the preshower prototype tests mentioned in previous sections. Therefore the part-time postdoc support requested here can be integrated perfectly with Prof. Zheng's existing research funding. In the case that the test results for the proposed one-year period are promising, Dr. Sulkosky may allocate more of his time to work on the EIC shashlyk calorimeter R&D at the next funding cycle. The graduate student involved will be Jie Liu, a 5th-year graduate student. Jie Liu will be supervised by Prof. Zheng and Dr. Sulkosky. The proposed work will be carried out in the Physics department at the University of Virginia.

## A The Method and the Potential of 3D-Printing

Because 3D printing is a relatively new technology and is not well known, we will describe in this section how 3D printing works in detail, and how it may be applied to shashlyk module construction.

Three-dimensional printing, also known as additive manufacturing (AM), is a process in which successive layers of material are laid down under computer control. These objects can be of almost any shape or geometry (hollow structure can be printed with a secondary supporting material that can be dissolved away after printing). The control can be provided from a 3D model or other electronic data source such as CAD drawings. Earlier AM equipment and materials were developed in the 1980s, but have only progressed rapidly in the past 5-10 years. Currently it is being used in a wide area of applications such as industrial prototyping, providing low-cost prototypes with fast turn-around time; high-tech development such as printing high-density lithium-ion batteries; printing medical shielding with highly-customized size and shape; in-home project construction by amateurs; and even educational projects in public schools, allowing teenage children to learn 3D construction and modeling and thus provide an interface for them to participate in higher-end research projects long before they enter college.

There are currently three kinds of 3D printing methods. The first is Fused Deposition Modeling (FDM), in which spools of plastic filament is melted when it approaches the tip of the printer and is printed on a supporting material. The supporting material is dissolved away after printing. The filament is typically made of thermoplastics such as acrylonitrile butadiene styrene (ABS) or polylactic acid (PLA), but can also be made of thermoplastics mixed with metal powder, providing a density up to  $4 \text{ g/cm}^3$ <sup>5</sup> used mostly for medical radiation shielding. For parts that requires transparency, acrylic-based material (“veroclear”) or the so-called “t-glase” material exist at a higher cost. In addition to commercially available filaments, one could extrude filaments in-house using custom extruders. Some people use in-house extruders to reduce the material cost of 3D-printing and to recycle plastics. We think it is also possible to experiment mixing plastic powder with metal powder and make our own high-density filaments. The second 3D printing technique is called poly-jet, in which liquid “ink” is printed from an inkjet-like printer head and then is UV-cured to the solid state. The third is for printing ceramic, pure metal or metal alloy. To print pure metal, metal powder is sintered (heated to just below melting point) either before or after printing. To sinter the metal powder before printing, an electron or a laser beam is typically used and the sintered powder is laid down in the desired 3D structure. To sinter the metal powder after printing, a binding material is printed on the powder by the printer, then loose powder is swept away and the bound powder is sintered in a furnace. This is called the “binder-jet” method.

For all three printing technique, the resolution varies from 0.1 mm for typical industrial-use printers, to slightly coarser ones for home and school uses, to  $16 \mu\text{m}$  for more higher-end models. The most commonly used 3D printers are the FDM type, with costs ranging from a few hundreds of US dollars to tens of thousands. Poly-jets and metal printers typically cost one and two orders of magnitudes more, respectively, than FDM printers of comparable specifications.

To 3D-print scintillators, one must formulate a 3D-printer compound from a plastic base with scintillating components. This technique is new and highly non-trivial (for an original study see Ref. [13]), and we will be working with Stratasys (a leading company in 3D printing) to develop scintillating compounds to use in polyjet printers. Their current formula produces scintillator pieces with similar light yield to EJ-204 (Eljen), and they are in the process of improving the mechanical strength of the product. The compound is only at the R&D stage and is not for sale, thus we will be obtaining only samples from Stratasys for the proposed study, at least in the first year.

We would like to point out two possibilities where the 3D-printing method can be particularly interesting for calorimeter construction. The first is a potentially simpler assembly procedure. Alignment pins can be printed using a different material at the same time as the scintillator sheets, and absorber layers (made from conventional methods) can be added by pausing the printer after each scintillator layer is printed. This procedure could be made automatic, and the only remaining steps

---

<sup>5</sup>This density is independent of the metal powder used. We do not know why higher density filaments are not available commercially.

of module assembly would be to compress the layers, to add endcaps, and to thread the WLS fibers. The second possibility is higher energy resolution. With the precision of 3D-printing and the fact that the cost is only proportional to the volume of the material and not the number of layers, one might expect construction of shashlyk modules made of ultra-thin layers without multiplying the cost. We would like to see how high energy resolution can be achieved.

With the advancement in 3D-printing one might also envision a final stage where the full shashlyk module can be printed on a 3D-printer. While it is unlikely that one can combine polyjets with metal-sintering, one could explore the possibility of mixing tungsten powder with thermoplastic or a liquid compound that reaches a density high enough to be used as the absorber. In this case, the full shashlyk module could be printed on a hybrid printer that combines FDM with poly-jet (although we still need to figure out how to add the reflective layers, if not manually). The layers can be aligned using alignment pins as described above. While this is certainly beyond the proposed funding period, it is an attractive goal and we will keep it in mind when carrying out the proposed R&D.

## References

- [1] A. Accardi, J. L. Albacete, M. Anselmino, N. Armesto, E. C. Aschenauer, A. Bacchetta, D. Boer and W. Brooks *et al.*, arXiv:1212.1701 [nucl-ex].
- [2] G. S. Atoian *et al.*, Nucl. Instrum. Meth. A **584**, 291 (2008).
- [3] Y. .V. Kharlov *et al.*, Nucl. Instrum. Meth. A **606**, 432 (2009).
- [4] D. A. Morozov *et al.*, J. Phys. Conf. Ser. **160**, 012021 (2009).
- [5] J. Allen *et al.* [ALICE EMCAL Collaboration], Nucl. Instrum. Meth. A **615**, 6 (2010) [arXiv:0912.2005 [physics.ins-det]].
- [6] C. Aidala, N. N. Ajitanand, Y. Akiba, Y. Akiba, R. Akimoto, J. Alexander, K. Aoki and N. Apadula *et al.*, arXiv:1207.6378 [nucl-ex].
- [7] S. Abeyratne, A. Accardi, S. Ahmed, D. Barber, J. Bisognano, A. Bogacz, A. Castilla and P. Chevtsov *et al.*, arXiv:1209.0757 [physics.acc-ph].
- [8] MEIC detector working group (JLab).
- [9] H. Huang *et al.*, Development of a new detector technology for fiber sampling calorimeters for EIC and STAR, EIC detector R&D proposal, 2011 and updates thereafter.
- [10] DIRC-based PID for the EIC Central Detector T. Horn, C. Hyde, P. Nadel-Turonski, J. Schwiening *et al.*, DIRC-based PID for the EIC Central Detector, EIC detector R&D proposal, 2011 and updates thereafter.
- [11] D. Green, The Physics of Particle detectors, Cambridge monographs on particle physics, nuclear physics and cosmology.
- [12] C. Grupen and B. Shwartz, Particle detectors, Cambridge monographs on particle physics, nuclear physics and cosmology.
- [13] Y. Mishnayot, M. Layani, I. Cooperstein, S. Magdassi and G. Ron, Rev. Sci. Instrum. **85**, 085102 (2014) [arXiv:1406.4817 [cond-mat.mtrl-sci]].